UNIVERSITY OF ALBERTA

THE CREATION OF T CELL HYBRIDOMAS TO MAP HUMAN GAD65 EPITOPES IN NOD MICE

by

HARBUKSH S. SEKHON ©

A thesis submitted to the Faculty of Graduate Studies and Research in partial fulfillment of the requirements for the degree of

MASTER OF SCIENCE

DEPARTMENT OF MEDICAL MICROBIOLOGY AND IMMUNOLOGY

Edmonton, Alberta

Fall 1998

National Library of Canada
Acquisitions and Bibliographic Services
395 Wellington Street
Ottawa ON K1A 0N4
Canada

Bibliothèque nationale du Canada
Acquisitions et services bibliographiques
395, rue Wellington
Ottawa ON K1A 0N4
Canada

Your file Votre référence

Our file Notre référence

The author has granted a non-exclusive licence allowing the National Library of Canada to reproduce, loan, distribute or sell copies of this thesis in microform, paper or electronic formats.

L'auteur a accordé une licence non exclusive permettant à la Bibliothèque nationale du Canada de reproduire, prêter, distribuer ou vendre des copies de cette thèse sous la forme de microfiche/film, de reproduction sur papier ou sur format électronique.

The author retains ownership of the copyright in this thesis. Neither the thesis nor substantial extracts from it may be printed or otherwise reproduced without the author's permission.

L'auteur conserve la propriété du droit d'auteur qui protège cette thèse. Ni la thèse ni des extraits substantiels de celle-ci ne doivent être imprimés ou autrement reproduits sans son autorisation.

0-612-34413-4

Canada

University of Alberta

Faculty of Graduate Studies and Research

The undersigned certify that they have read, and recommend to the Faculty of Graduate Studies and Research for acceptance, a thesis entitled **The Creation of T Cell Hybridomas to Map Human GAD65 Epitopes in NOD Mice** submitted by **Harbuksh Singh Sekhon** in partial fulfillment of the requirements for the degree of **Master of Science**.

Dr. John F. Elliott

Dr. Kevin P. Kane

Dr. David Rayner

Dr. Mark Peppler
(Chair of the Examining Committee)

Dated: May 4/98

ABSTRACT

Insulin-dependent diabetes mellitus is an autoimmune diseases in which autoreactive T cells play a pivotal role in pathogenesis by mediating the destruction of insulin-producing-cells in the islets of Langerhans of the pancreas. Non-obese diabetic mice develop diabetes spontaneously and closely mimic the human disease, establishing them as a useful model in studying underlying disease mechanisms. The first part of this study focuses on the development and characterization of T cell hybridomas from non-obese diabetic mice that respond to human glutamic acid decarboxylase 65 (hGAD65), an important autoantigen in diabetogenesis. One hybridoma recognized the hGAD65 epitope spanning amino acids 551-570. The second part of this study examines the potential use of green fluorescent protein (GFP) as a marker of activation in T cell hybridomas, by stably transfecting the GFP reporter gene coupled to an IL-2 related promoter into the fusion partner.

For my parents and family.

TABLE OF CONTENTS

	Page
Chapter I - Introduction	
The Immune System	1
The Human Leukocyte Antigen Complex	1
HLA Class I and Class II Structure	3
Assembly of Class I and Class II Molecules	5
T Cell Receptor Structure	7
T Cell Activation	8
HLA Disease Association	11
Insulin-Dependent Diabetes Mellitus	11
Mechanisms of Autoimmunity	13
Autoantigens in IDDM	16
Animal Models of IDDM: Non-Obese Diabetic Mice	21
Experimental Design	21
Chapter II - Materials and Methods	
PCR	24
Clean Up of PCR Products, Restriction Enzyme Digestion, and ligation	25
Transformation of *E.coli*	26
Plasmid DNA Preparation	27
Cell Culture	29
Immunization of Mice	29
Isolation and Culture of Lymph Node Cells	29
T cell Hybridoma Production	30
T cell Stimulation	31
IL-2 ELISA	32
FACScan/FACSort	32
Electroporation of Plasmid DNA	33
Propidium Iodide Staining of T Cells	33

Chapter III - Characterization of NOD-Restricted T Cell Epitopes to Human Glutamic Acid Decarboxylase 65 Using T Cell Hybridomas

Introduction..... 35

Results and Discussion..... 37

Conclusions..... 28

Future Directions..... 40

Chapter IV - The Use of GFP Coupled to a Minimal IL-2 Promoter/Enhancer to Study T cell Activation

Introduction..... 46

Results and Discussion..... 49

Conclusions..... 55

Future Directions..... 56

Chapter V - General Discussion and Conclusions..... 71

Bibliography..... 74

LIST OF TABLES

Table	Description	Page Number
2.1	Oligonucleotides used in the course of cloning	
3.1	IL-2 produced by NOD-restricted, hGAD65-specific T cell hybridoma lines and daughter clones	
3.2	Sequences of overlapping peptides to hGAD-65	
3.3	IL-2 produced by NG 17.5 recognition of $hGAD65_{551-570}$	
3.4	Presence of a defined $I\text{-}A_g^{g7}$ peptide-binding motif within NOD-restricted, hGAD65 T cell epitopes	
4.1	IL-2 produced by NOD-restricted, OVA-specific T cell hybridomas	

LIST OF FIGURES

Figure	Description	Page Number
1.1	The HLA Complex	
3.1	Comparison of sequence identity between $hGAD65_{551-570}$ and its corresponding sequence in mGAD65 and mGAD67	
4.1	Schematic of $NFAT_3$-Lac Z reporter construct	
4.2	Schematic of fluorescence production in *Aequoria victoria*	
4.3	The pSRαSD7-GFP65T vector	
4.4	The p5'IL2-GFP65T vector	
4.5	The $pNFAT_3$-GFP65T vector	
4.6	Change in BW α–β– cell viability and cloning efficiency with increasing electroporation voltages	
4.7	GFP induction in BW α–β– stably transfected with different GFP-containing vectors	
4.8	SSC-H vs FSC-H plot of T cells stimulated with PMA/ionomycin	
4.9	PCR-detection of GFP gene retention in NOD-restricted, OVA-specific T hybridoma lines 6 and 8	
4.10	sFasIg does not appreciably decrease AICD in PMA/ionomycin stimulated T cells	
4.11	GFP is not detectable in OVA-specific T hybridomas produced by fusion with the NFAT 5.5 fusion partner	
4.12	SSC-H vs FSC-H plot of OVA-specific T cell hybridomas stimulated with PMA/ionomycin	

LIST OF ABBREVIATIONS

aa	amino acids
APL	altered peptide ligand
ABTS	2,2'-azino-bis (3-ethylbenz-thiazoline-6-sulfonic acid)
AICD	activation-induced cell death
APC	Antigen presenting cell
ATP	adenosine triphosphate
β_2M	beta-2 microglobulin
BB	bio-breeding
BSA	bovine serum albumin
C	constant
cDNA	complementary deoxyribonucleic acid
CDR	complementary determining region
CFA	complete Freund's adjuvant
CLIP	class II associated invariant chain peptide
cm	centimeter
CO_2	carbon dioxide
CPG	controlled pore glass
CsCl	cesium chloride
D	diversity
DAG	diacylglycerol
DNA	deoxyribonucleic acid
dNTP	deoxynucleotide triphosphate
dsDNA	double stranded DNA
EDTA	ethylene diamine tetracetic acid, pH 8.0
ELISA	enzyme-linked immunosorbent assay
ER	endoplasmic reticulum
EtBr	ethidium bromide
EtOH	ethanol
FACS	fluorescent activated cell sorter
FCS	fetal calf serum
FSC	forward scatter
GAD	glutamic acid decarboxylase
GFP	green fluorescent protein

H_20	deionized, distilled water
HBS	HEPES-bufferd saline
HBSS	Hank's buffered salt solution
hGAD65	human glutamic acid decarboxylase 65 kD isoform
HLA	human leukocyte antigen complex
HRP	horseradish peroxidase
ICAM	intercellular adhesion molecule
IDDM	insulin-dependent diabetes mellitus
IFN	interferon
Ig	immunoglobulin
Ii	invariant chain
IL-2/IL-2R	interleukin 2/interleukin 2 receptor
IP_3	phosphotidylinositol 1,4,5-triphosphate
ITAM	immunoreceptor tyrosine-based activation sequence motifs
J	junctional
KOAc	potassium acetate
lacZ	bacterial betagalactosidase
LB	Luria-Bertani
LFA	Lymphocyte-function associated antigen
$MgCl_2$	magnesium chloride
MHC	major histocompatibility complex
µF	micro Faradays
MIIC	MHC class II compartments
min	minutes
ml	milliliter
MS	multiple sclerosis
NaOAc	sodium acetate
NaOH	sodium hydroxide
NFAT	nuclear factor of activated T cells
$(NH_4)_2SO_4$	ammonium sulfate
NOD	non-obese diabetic
OVA	chicken egg ovalbumin
PBMC	peripheral blood mononuclear cells
PBS	phosphate-buffered saline
PBST	phosphate-buffered saline supplemented with 0.05% Tween 20

PCR	polymerase chain reaction
PEG	50 % polyethylene glycol in PBS (molecular weight 1500 daltons)
PI	propidium iodide
PIP_2	phosphotidylinositol 4,5-bisphosphate
PKC	protein kinase C
PMA	phorbol 12-myristate 13-acetate
Pfu	*Pyrococcus furiosus*
RNA	ribonucleic acid
RNAse A	ribonuclease A
rpm	revolutions per minute
SDS	sodium dodecyl sulphate
sec	seconds
sFasIg	soluble Fas immunoglobulin fusion protein
SM	staining medium
SSC	side scatter
ssDNA	single stranded DNA
TAE	tris-acetate buffer
TAP	transporter associated with antigen processing
Taq	*Thermus aquaticus*
TBE	tris-borate buffer
TCR	T cell receptor
TE	tris-EDTA
Tris-HCl	tris-hydrochloride
V	variable

Chapter I

INTRODUCTION

The Immune System

The human immune system responds to pathogenic insults in an inherently specific and concerted fashion, utilizing both the humoral and cellular branches of immunity. While the immune system has developed to favour the clearance of non- or aberrant-self cells or substances, it is occasionally stimulated to mount a response to apparently normal cells. Such autoimmune destruction can be mediated humorally through antibodies secreted by B lymphocytes that recognize conformational epitopes on native antigen. Alternatively, or in conjunction with autoantibodies, cellular damage occurs through T lymphocytes whose T cell receptor recognizes linear fragments of denatured antigen presented in association with primarily one of two specific products of the human leukocyte antigen complex.

The Human Leukocyte Antigen Complex

The human leukocyte antigen (HLA) complex, located on the short arm of chromosome 6, was originally discovered in the 1950's in the sera of multiply transfused patients (1). The HLA complex is composed of three main gene families, referred to as class I, II, and III (2; Figure 1.1). Class I, divided into the A, B, and C loci, and class II, consisting of DP, DQ, and DR loci, are characterized by extensive allelic polymorphism manifesting as variation in amino acid composition (3). The structural diversity of the class I and II gene products have important implications for the functional interaction of HLA molecules with T cells and the ensuing immunological response.

HLA class I molecules are type I integral membrane proteins encoded within the class I region, spanning approximately 1600kb at the telomeric end of the chromosome (4).

HLA class I genes encode the α chain of class I molecules. Thus, α chains encoded by HLA-A, -B, and -C associate with an invariant second chain, β_2-microglobulin (β_2M), to form functional class I heterodimers (5). β_2M is a non-major histocompatibility complex (MHC) encoded protein, localizing to chromosome 15 in man (6). Three additional loci, E, F, and G, encode non-classical class I proteins capable of associating with β_2M(7,8).

Class II molecules are heterodimeric integral membrane proteins encoded within the most centromeric 900kb region (4,9). Both the α and β chains of class II heterodimers are encoded on the same chromosome and within the same region. Three loci, DP, DQ, and DR, are responsible for encoding the class II α and β gene products. The DP subregion includes two different α (DPA1 and DPA2) and β (DPB1 and DPB2) genes (2), of which the combination of DPA1/DPB1 encodes functional DP heterodimers. DPA2 and DPB2 are both pseudogenes that do not give rise to transcripts (10). Of the different DQ genes, only DQA1 and DQB1 produce heterodimers with the serological specificity DQ1-9; DQA2, DQB2 and DQB3 are pseudogenes that are not expressed (2). The DR region encodes a non-polymorphic DRA gene that codes for the α chain and nine different β chain DRB genes, of which DR2, 6, 7, 8, and 9 are pseudogenes. The DR1 and DR8 group haplotypes each carry only one functional DRB gene, DRB1, of serological specificities DR1-18. The remaining group haplotypes, DR51, 52, and 53, carry DPB1 with one other functional DRB gene, either DRB3, 4, or 5, which give rise to the DR52, DR53, and DR51 serological specificities, respectively (4). The class II region also contains the TAP1/2 and LMP2/7 genes that are associated with the processing of protein and transport of peptides from the cytosol to the lumen of the endoplasmic reticulum (ER) (11).

The HLA complex is marked by recombination between its various loci. The frequency of recombination between certain subregions, however, exceeds the normal

expected frequency. Such linkage disequilibrium occurs often between DR and DQ, which are located within 80-300kb of one another, but less often between DQ and DP due to the intervening 800kb (12). It has been postulated that the observed association between particular loci may reflect either insufficient evolutionary time to permit loci to reach equilibrium or the inheritance of a selective advantage in the combination of two particular alleles (13).

HLA class I glycoproteins are expressed on the surface of most nucleated somatic cells. Class II molecules are present primarily on cells involved in the presentation of antigen to CD4+ T cells, such as B cells, macrophages and dendritic cells, as well as on capillary endothelium (14, 15). Class II expression has also been noted in cases of inflammation on cells that do not constitutively express class II (16). Interferon gamma, in particular, has been shown to induce expression of class II molecules in cells such as fibroblasts, which do not normally express class II, through the action of a class II transactivator (17).

HLA Class I and Class II Structure

i) Class I

HLA class I molecules are type I integral membrane proteins consisting of a heterodimeric 46kd α heavy chain non-covalently associated with a conserved 12kd β_2M light chain. The heavy chain consists from the N-terminus of α_1, α_2, and α_3 domains followed by a transmembrane and short cytoplasmic region (18). The non-MHC encoded β_2M light chain and the α_3 domain of the heavy chain that it interacts with are structurally homologous to immunoglobulin (Ig) constant region domains, folding to form Ig-like domains (19). Consequently, class I molecules are considered part of the Ig gene superfamily. X-ray crystallographic analysis of HLA-A2 and -Aw68 has revealed that the

α_1 and α_2 domains fold to form a putative peptide binding site consisting of walls of two parallel α-helices and a floor of eight antiparallel β-pleated sheets which can accommodate peptides of 8-10 amino acids in length (20, 21). Importantly, the polymorphisms associated with individual HLA allelic products are localized to those portions of the α-helical walls and β -pleated sheets that face the peptide binding groove and interact with antigenic peptides. Further structural analysis of viral peptides bound to crystallized class I molecules revealed that the importance of allele-specific pockets that may extend deep between the floor and helical walls of the binding domain (22). Conceptually, polymorphic residues on the surface of the groove and those which extend into the pockets are able to influence the panel of peptides that are able to bind to a specific HLA class I molecule by influencing the size, shape and biochemical properties of the peptide binding groove.

ii) Class II

Class II molecules are heterodimeric integral membrane proteins consisting of a 29 to 33kd α chain non-covalently associated with a 24 to 29kd β chain. Both chains consist of two domains which, from the N-terminus, are α_1 and α_2 for the a chain and β_1 and β_2 for the β chain (9). The α_2 and β_2 domains are homologous to Ig constant domains and class II molecules are therefore members of the Ig gene superfamily (23). X-ray crystallographic analysis of HLA-DR1 has shown that the α_1 and β_1 domain of the class II molecule fold in a manner analogous to the α_1 and α_2 domains of class I molecules, forming a similar peptide binding cleft (24). However, in contrast to class I molecules, the class II groove is able to accommodate peptides of 12-24 amino acids in length (25-27), possibly due to the fact that class II groove openings are not occluded by amino acid side chains (24).

Assembly of Class I and Class II Molecules

Newly synthesized class I heavy chains that are cotranslationally translocated into the ER are bound by a Ca^{2+}-sensitive, ER-resident protein termed calnexin (28). Calnexin appears to facilitate folding and disulfide bridge formation of nascent heavy chains well as the actual assembly of heavy chains with β_2M (29). Recent research has suggested that upon binding of β_2M, the class I heterodimer dissociates from calnexin, and forms a new complex with calreticulin, tapasin, and the transporters associated with antigen processing (TAP 1/TAP 2) (30). TAP 1/TAP 2 are responsible for the transport of cytosolic peptides of 8-10 amino acids in length, generated in the cytosol from intracellularly-derived proteins cleaved by the multicatalytic proteasome complex (31). The trimolecular complex of heavy chain, β_2M and peptide are transported through the medial and trans-Golgi where they follow the exocytic pathway of cell surface expression (32).

The α and β chains of class II HLA molecules associate with a non-polymorphic, or invariant (Ii) chain once they enter the ER (33). Ii is a type II transmembrane protein that exists in at least four forms as generated by differential translation and/or alternative exon splicing (34). Ii associates with α and β chains to form an initial core trimer in the ER which in turn associates with more α and β chains to form a nonameric complex $[(\alpha\beta Ii)_3)]$ that is incapable of binding antigenic peptides (35, 36). The $(\alpha\beta Ii)_3$ complex moves through the medial and cis-Golgi like class I, until it reaches the trans-Golgi network, where a di-leucine based targeting signal redirects the class II molecule from the secretory pathway to endocytic compartments or specialized compartments in antigen presenting cells (APCs) referred to as MHC class II compartments (MIIC's) (37). Within these compartments, Ii is degraded by resident enzymes, leaving behind a class II associated invariant chain peptide (CLIP) within the class II peptide-binding groove, corresponding to

Ii amino acids 81-104 (38, 39). HLA-DM, another MIIC-resident HLA-encoded protein, catalyzes the removal of CLIP in exchange for antigenic peptide (40, 41). Class II-peptide complexes are then transported to the plasma membrane for presentation to T cells.

Immunological dogma held that class I/II molecules utilize mutually exclusive sources of antigenic peptides. Class I were thought to exclusively present intracellularly-derived antigen while class II were believed to present antigens of exogenous origin that gain entry into the antigen processing pathway via a cell's endocytic sampling of its extracellular environment (42). These observations were based largely on the isolation, sequencing, and identification of peptides naturally associated with isolated class I and II molecules (43-47). The division of labour amongst the two HLA classes was further supported by the use of the pharmacologic agents chloroquine, which neutralizes the low pH normally found in endosomal compartments, and Brefeldin A, a fungal product which blocks the egress of newly synthesized secreted and plasma membrane proteins from the ER. Three important conclusions were drawn from the effect of these agents on antigen processing and presentation pathways; first, chloroquine was found to block only class II antigen presentation (48), suggesting that class II antigen may associate with antigen in endosomal compartments, a retrospectively logical assumption based on the endosomal sorting signal associated with the invariant chain. Second, Brefeldin A was found to inhibit only class I antigen processing, indicating that class I-restricted peptides associate with newly synthesized class I in the lumen of the ER (49). The mutually exclusive actions of these two inhibitors on class I and II pathways lends itself to the idea that both antigen presentation molecules may utilize distinct presentation pathways that rely on unique pools of proteins. However, the distinction between these two pathways is not absolute, such that exogenous proteins have been found associated with class I restricted responses and vice-versa (50-52). In fact, specialized APCs like macrophages and dendritic cells are capable of providing exogenously-derived proteins to class I molecules for presentation.

Generally, though, it is accepted that newly synthesized class I molecules in the ER are provided with peptides of endogenous origin from within the cytosol. Class II molecules acquire their antigens from the extracellular milieu as endocytosed complex antigens that are degraded in acidic endosomes and which subsequently fuse with class II-containing endosomes (18).

T Cell Receptor Structure

T lymphocyte responses to foreign antigen are governed by the surface T cell receptor (TCR), consisting of one of two variants of a heterodimeric glycoprotein: αβ or γδ (53-54). Each of the four chains contains an amino terminal variable region, incorporating hypervariable areas analogous to the complementary determining regions (CDRs) of immunoglobulin molecules, with each chain having three CDRs (55). The membrane proximal constant domain is identical amongst each of the chains. Both the variable and constant domains of each chain contains a disulfide bond between cysteine residues that forms an immunoglobulin fold or domain (54). All chains share a short, cysteine-containing sequence that is involved in interchain disulfide linking of the two members of a TCR heterodimer. A transmembrane region of positively charged amino acids allows for effective association with other membrane proteins involved in TCR-mediated signalling events. The carboxy-terminal end of each chain is represented as a short, cytoplasmic tail (56).

The TCR is encoded by gene segments encoding variable (V), diversity (D) and joining (J) elements that rearrange in thymocytes and are brought into close proximity with the constant (C) region gene segment (57). The α chain is encoded by joining of V, J and C, while the β chain is produced from V, D, J, and C segments. The combination of these different segments, along with alternative joining of D gene segments for β chains,

junctional flexibility, and N- and P-region nucleotide addition, contribute to the vast diversity of the TCR (56). The V gene segment encodes the CDR1 and CDR2 regions of the TCR and are less diverse then their Ig counterparts due to fewer TCR V region genes. In contrast, the CDR3 region is much more diverse than the Ig CDR3 region, owing to the aforementioned mechanisms of generating TCR diversity. This led to the hypothesis that CDR3 sequences were principally involved in the recognition of highly variable side chains within the antigenic peptide while CDR1 and CDR2 interact with MHC α-helices (57, 58). Recently, this model was confirmed by analysis of the X-ray crystal structure of a TCR bound to a class I-peptide complex (59).

Rearranged TCRs expressed on the surface of thymocytes are then subject to positive and negative selection within the thymus. Positive selection, which occurs between naive thymocytes expressing rearranged TCR and thymus cortical epithelial cells, selects for those T cells that are capable of recognizing self MHC (60, 61). Negative selection between thymocytes and either macrophages or dendritic cells results in the elimination of T cells capable of recognizing self antigens in the context of self MHC (62).

T Cell Activation

T cell activation is mediated by TCR recognition of antigen-MHC complexes, however it is not solely a function of TCR-mediated signal events; rather, it is thought to involve two signals with engagement of the TCR by peptide/MHC complexes on antigen presenting cells transducing the first signal and costimulatory ligands present on APCs providing the second signal through cognate receptors present on the T cell (63, 64). Thus, the initial events in T cell activation can be divided into three phases: (1) antigen-independent cell adhesion, (2) TCR recognition of the peptide-MHC complex, TCR-dependent strengthening of cell adhesion, and TCR-mediated signalling events (3) costimulation via specific adhesion receptor-ligand pairs (65).

The ability of a particular TCR to recognize class I or II molecules is regulated by the mutually exclusive surface expression of one of two surface glycoproteins, CD4 and CD8. CD4 is a monomeric glycoprotein with four external immunoglobulin domains of which the two most membrane distal recognize non-polymorphic residues in the β_2 domain of class II on APCs while the two most membrane proximal immunoglobulin domains interact with the TCR (66, 67). CD8 consists of either a homodimeric α/α or heterodimeric α/β glycoprotein that recognizes non-polymorphic residues on the α_3 domain of class I-bearing APCs (68). CD4 and CD8 also increase the avidity of the interaction between TCR and peptide/MHC, which is at best a low affinity interaction (65), and are essential to TCR/CD3-mediated signal transduction (69).

T cell recognition of antigenic peptide in the context of MHC results in a cascade of signalling events that culminates in the activation of the T cell. Signal transduction requires the association of a complex of proteins, collectively designated CD3, with the TCR (70). The α and β chain of the TCR each have short, five amino acid cytoplasmic tails which do not serve as substrates for known protein kinases. The polypeptide chains γ, δ, ε, and ζ, combinations of which comprise CD3, contain immunoreceptor tyrosine-based activation sequence motifs (ITAMs) within their cytoplasmic domains (71). Upon antigen recognition, CD45, a protein tyrosine phosphatase activates two *src* related kinases, an $\alpha\beta$ -associated *fyn* kinase ($pp59^{fyn}$) and a CD4/8-associated lck kinase ($pp56^{lck}$) (64-66), by dephosphorylation of negative regulatory domains in each kinase. These kinases then phosphorylate tyrosine residues within ITAMs of the ε and ζ chains of CD3. A third kinase, ZAP-70, is recruited to the phosphorylated ζ chain and, together with *fyn*, mediate tyrosine kinase phosphorylation and activation of phospholipase Cγ1 (PLC-γ1) (72).

PLC-γ1 activation mediates cleavage of phosphotidylinositol 4,5-bisphosphate (PIP_2) to the soluble intracellular messenger phosphotidylinositol 1,4,5-triphosphate (IP_3) and diacylglycerol (DAG), the endogenous lipid stimulator of protein kinase C (PKC) (66,67). IP3 causes an increase in intracellular calcium concentration that, in combination with calmodulin, activates the serine/threonine protein phosphatase calcineurin. Calcineurin subsequently acts on nuclear factor of activated T cell (NFAT), dephosphorylating the cytoplasmic subunit of NFAT. Activated PKC causes the phosphorylation of other cellular proteins that mediate the dephosphorylation of another nuclear factor, NF-κB. NF-κB and NFAT then enter the nucleus, where the cytoplasmic subunit of NFAT is then able to combine with its nuclear subunit (73). Binding of these factors, along with others, to the IL-2 promoter region results in transcription and translation of the IL-2 gene and expression of the IL-2 receptor (IL-2R) (74), which is ultimately necessary for T cell progression from initial activation to DNA synthesis and clonal expansion (75).

T cell costimulation is mediated primarily by CD2, LFA-1, and CD28 on T cells though their interaction with LFA-3, ICAM-1, and B7, respectively, on APCs. CD2 is expressed on all T cells while its ligand, LFA-3, is much more broadly expressed (76, 77). The LFA-3/CD2 pathway initiates strong antigen-independent cell adhesion and expansion of naive T helper cells (65). CD28 is constitutively expressed on T cells and is thought to be the primary T cell costimulator. There are two variants of its B7 counter-receptor: B7-1(CD80) and B7-2(CD 86) which are differentially expressed. B7-1 is absent on resting APC, but is induced late in an immune response while B7-2 is constitutively expressed on unstimulated B cells, dendritic cells, and monocytes and is further upregulated during an immune response (78-80). CD28-B7 interaction is thought to exert its costimulatory activity either through induction of a novel CD28RC DNA binding protein (81) or through

IL-2 message stabilization. LFA-1 is expressed on lymphocytes, monocytes, macrophages, and with increased levels on memory T cells. Its primary ligand with respect to T cell activation is ICAM-1 (82). LFA-1 is transiently induced to a higher affinity state by ligation of the TCR or CD2 (83). LFA-1/ICAM-1 interactions are important mediators of adhesive interaction between the T cell and APC. These accessory molecules are necessary to increase the avidity of the interaction between T lymphocytes and APC's, ensuring optimized TCR occupancy and subsequent signal transduction (69).

HLA Disease Association

Individual haplotypes and/or loci of the HLA complex have been found to be associated with the occurrence of certain diseases. The level of association between a particular disease and an allele at one of the MHC loci is often defined by the relative risk, or frequency of disease in individuals who have the antigen compared to frequency in individuals who lack the antigen (84). A relative risk greater than 1 is thought to indicate an association between a specific disease and antigen. Notable examples include ankylosing spondylitis in which the HLA-B27 allele has been assigned a relative risk of 87.4, celiac disease with a relative risk of 10.8 linked to DR3, and insulin-dependent diabetes mellitus, for which a causal link to specific DR haplotypes and DQ alleles has been suggested, although the relative risk varies between ethnic groups.

Insulin-Dependent Diabetes Mellitus

Insulin-dependent diabetes mellitus (IDDM) results from autoimmune destruction of insulin producing pancreatic β-cells (85). Immunopathology reveals mononuclear cell infiltrates and chronic inflammation. T lymphocytes are thought to play a pivotal role in diabetogenesis (86). As with many autoimmune diseases, IDDM has been associated with particular alleles of the HLA complex and several putative autoantigens have been

implicated in eliciting both autoreactive antibody and T cell responses (87-89).

Attempts to identify the exact gene(s) associated with IDDM have been unsuccessful thus far owing not only to linkage disequilibrium, but to the complex and often variable association of several HLA alleles with IDDM. IDDM was initially linked to HLA class I B8 and B15, followed by DR3 and DR4 which are in linkage disequilibrium with B8 and B15 respectively (90). Amongst Caucasians with IDDM, 95% of individuals are HLA DR3 or DR4 as compared to 40% of the general population (91). Further complexity arises from the mechanism of DQ heterodimer formation which may be encoded in cis (on the same haplotype) or trans (on different haplotypes) (92). Thus for a homozygous individual, only one possible heterodimer can be expressed on the cell surface. A heterozygous individual may express up to four different DQ antigens of the cell surface.

Recently, attention has focused on individual DQB1 alleles as markers of susceptibility. Nepom *et al* identified a specific DQβ variant, DQB1*0302, found in more than 90% of DR4-positive IDDM patients (93). While the expression of DQB1*0302 is highly associated with IDDM, it is apparent that it may be a necessary although insufficient component for the onset of disease, as DQB1*0302 was found to be expressed in a non-IDDM, DR4-positive sibling of an afflicted individual. Specific DQ heterodimers have been associated with diabetes susceptibility and resistance. A varying degree of susceptibility or resistance is thought to be conferred by these DQ molecules with DQ resistance molecules being dominant over those which predispose to the disease (reviewed in ref. 94). Susceptibility in Caucasians, Blacks, and Japanese is most often associated with DQ2 (DQA1*0501, DQB1*0201) when the haplotype is DR3-DQ2 and DQ8 (DQA1*0301, DQB1*0302). DQA1*0301/DQB1*0201, encoded in cis on DR7 in Blacks and in trans for DR3-DQ2/DR4-DQ8 heterozygous Caucasians was found to be

significantly associated with increased risk. DR3-DQ2/DR4-DQ8 heterozygotes are at a particularly high risk of developing IDDM, a finding that can be explained by such an individual's ability to generate up to four different DQ molecules that are each associated with increased susceptibility. In Japanese IDDM patients, genetic predisposition is also associated with DQ4 (DQA1*0301, DQB1*0401) and DQ9 (DQA1*0301, DQB1*0402). Thorsby and Ronningen note that while these two haplotypes are rare amongst Blacks and Caucasians, a weak although significant association can be found in the trans-encoded DQA1*0301, DQB1*0402 heterodimer (94). Since the DQB1*0401 and *0402 genes differ only at codon 23, nearly identical DQ molecules are expressed.

Todd *et al* suggested that the identity of the amino acid at position 57 of the DQβ chain was a major determinant of susceptibility of resistance based on the observation that a lack of aspartic acid was associated with disease (95). Thus, the presence of Asp_{57} would impart resistance and non-Asp_{57} was associated with susceptibility. However, epidemiological data has shown that the presence or absence of position 57 identity is in itself not a sufficient marker of diabetes predisposition (96-98).

Mechanisms of Autoimmunity

In considering the mechanism of action of a cell-mediated autoimmune disease, one has the advantage of being able to operate within a framework that is built around the understanding of the molecular rules and processes that regulate T lymphocyte actions. An individual's T cell repertoire is established at birth by thymic education in which T cells capable of recognizing self-HLA molecules are positively selected while self-HLA restricted T cells capable of recognizing self antigen are deleted from the developing pool of TCR specificities (99). The fact that circulating T cells capable of recognizing self-derived peptides and destroying an individual's insulin-producing β-cells are present in IDDM

demonstrates that self-tolerance is circumvented, implicating inadequate self-tolerance as a possible mechanism. IDDM is not a universal disease in that specific individuals with particular HLA class II genes are genetically predisposed to the disease, although they may not always develop disease. However, the strong association with DR haplotypes suggests a role for these HLA allele products in aberrant negative selection. Thymic education is based on the principle that T cells capable of strongly binding to self proteins in the context of self-HLA are targeted for elimination in the thymus. Thus, avidity is a central issue in the establishment T cell self-tolerance (100). The fact that T cells generally do not recognize empty HLA molecules argues that the removal of self-reactive T cell clones would necessarily require presentation of self-peptide with class II. The presence, then, of self-reactive T cells may suggest inadequate presentation of putative diabetogenic self-peptides to T cells in the thymus. The fact that the spectrum of potential autoantigens in both normal and IDDM-destined individuals are identical at the time of thymic education (i.e. both groups produce insulin, hGAD65, and other suspected autoantigens) indicates that the breakdown in negative selection is not a feature of binding characteristics mediated by the peptide itself; rather, the peptide binding qualities of the individual class II HLA gene products that have been associated more with IDDM patients than the general population are more likely candidates.

A model that reflects the central role of the class II HLA DQ genes in IDDM etiology has been presented by Nepom (101). The model is based on differences in affinity of different HLA-DQ heterodimers for self-derived peptides. Nepom contends that the unique polymorphic residue composition of the individual DQ elements manifests itself in a varying ability to bind normally tolerizing peptides, ultimately conferring either susceptibility or resistance to a particular individual. However, Nepom suggests that this is a peripheral effect, presenting at the level of immunogenic peptide binding to class II molecules in late endosomes. The binding of a particular peptide with DQ6, for instance,

may then be proposed to lead to T cell anergy when expressed on the surface of the APCs. The corollary is that binding of peptide to DQ2 or DQ8 is not as efficient, precipitating the diabetic state.

One should note that this model presupposes the existence of autoreactive T cells in the periphery. The presence of such T cells must be reconciled with the current understanding of thymic education and progression to autoimmunity, whether it be IDDM or multiple sclerosis. A recent review by Theofilopoulos proposes that organ specific sequestration of antigens may prevent the exposure of potential autoantigens to T cells undergoing central selection, supporting the establishment of autoreactive T cells in the periphery and the possibility of a subsequent autoimmune episode (102). Although this theory appears plausible, it does not seem likely that peptides derived from GAD would not be presented to cells in the thymus, in light of its identification in neurons and as a target of autoreactive T cells.

In this sense, molecular mimicry becomes an attractive theory in its ability to, at least theoretically, unify the autoimmune state with successful negative selection. The antigen/HLA specificity of a particular TCR, specific for a peptide derived from coxsackie virus may require the presence of particular anchor residues or motifs within the linear peptide sequence. The presentation of DQ-restricted, hGAD65-derived peptides on the APCs may conceivably elicit a response from that T cell if specific core amino acids are shared between the viral- and enzyme-derived peptides. A non-sequential, seven amino acid homology sequence has been shown to exist between hGAD65 and the P2-C protein of coxsackie B4 virus (103, 104). To date, no report has been made on differences or similarities in peptide binding motifs for DQ2, 6, or 8, with respect to putative autoantigens.

A second argument discussed by Theofilopoulos is the cryptic self hypothesis, based on the molecular rather than anatomic sequestration of peptide determinants. This

theory is based on negative selection occurring through the presentation of a small subset of high affinity, well-displayed determinants from self-peptides to T cells. A population of T cells, then, is thought to exist which has not been tolerized to subdominant, or cryptic, determinants. The existence of such epitopes may have two readily observable implications for antigen processing in the context of IDDM. First, differential expression of self-epitopes by dendritic and/or epithelial cells as compared to B lymphocytes may account for differences in the presentation of dominant/sub-dominant epitopes. This may in fact be due to the professional APC designation accorded to dendritic cells, as well as the randomness associated with immunogenic peptide generation. Alternatively, antigen processing could be similar in both cell types, but the immunodominant epitopes may be several times more competitive than the cryptic determinants in binding to particular HLA-DQ molecules. This is a variation on the hypothesis that the differing DQ molecules have different affinities for the same peptide at the level of negative selection. In order to account for the HLA associations with IDDM, it could be possible that resistance alleles are able to bind tolerizing, dominant epitopes, releasing only non-auto-reactive cells that do not recognize sub-dominant epitopes. Susceptibility may therefore reflect the inability of DQ2 or DQ8 to bind a subdominant, tolerizing epitope. Thus, dominancy/crypticity may be a function of the HLA allele itself.

Autoantigens in IDDM

Newly diagnosed IDDM patients have been found to have circulating autoantibodies to a number of islet-cell-derived antigens (75,76). Peripheral blood mononuclear cells (PBMCs) from IDDM patients have been shown to proliferate in response to specific islet-derived antigens, supporting the involvement of T lymphocytes in diabetogenesis. Descriptions of some of the autoantigens implicated in cellular recognition are presented below.

i) *Glutamic acid decarboxylase*

Glutamic acid decarboxylase (GAD) was initially visualized, although not identified, as a 64kd protein that could be immunoprecipitated from islet detergent lysates using sera from IDDM-afflicted individuals (105). Subsequently, the 64kd protein was identified as GAD (106). GAD exists in two forms with molecular masses of 65 (GAD65) and 67kd (GAD67) sharing approximately 70% sequence homology. Each form is encoded by a different gene located on different chromosomes; GAD65 on chromosome 2 and GAD67 on chromosome 10 in man (107). Islet GAD, through its production of γ-amino butyric acid, is thought to play a role in the inhibition of somatostatin and glucagon secretion, as well as in regulating insulin secretion and proinsulin synthesis (89, 108). GAD65 is thought to be both the predominant form of GAD in the islet cell and the principle version targeted in IDDM in man, whereas GAD67 (a highly homologous protein) plays this role in the non-obese diabetic (NOD) mouse (109, 110).

Recently, it has been demonstrated that in the NOD mouse model, insulitis was associated with the presence of a cell-mediated response to hGAD65 (111-113). A class II-restricted proliferative response to hGAD65-derived peptides was observed. Intrathymic injection of GAD65 was shown to significantly decrease the occurrence of diabetes. Several groups have attempted to identify the immunodominant epitopes that are being recognized by T cells by overlapping-peptide mapping studies in which the ability of human PBMCs (from both diabetics and non-diabetics) to respond to specific portion of hGAD65 is analyzed. Peptides corresponding to positions 247-269, 260-279, and 473-455, of hGAD65 have been independently identified as possible immunodominant epitopes (114, 115).

ii) *Coxsackie B4 Virus: P2-C Protein*

Coxsackie virus was isolated from the pancreas of a child with diabetic ketoacidosis more than fifteen years ago (116). Since that time, several groups have demonstrated that coxsackie B4 virus can induce diabetes in both non-human primates and mice (117, 118). Circulating antibodies to viral proteins have also been reported to exist in children with IDDM (119, 120).

Coxsackie B4 virus is thought to be an environmental trigger for IDDM. The virus' 40kd P2-C protein has shares a short, six amino acid region of homology in the region of residues 32-47 with amino acids in the 255-269 position of hGAD65. Tian *et al* found that out of ten different strains of mice tested, a T cell response to the hGAD65 and the P2-C sequence similarity peptides could only be induced in NOD mice (104). Further, responses of T cell lines derived from immunization with either hGAD65 or P2-C homology peptides could be recalled when stimulated with the other peptide. The fact that Atkinson *et al* has also reported proliferative responses with PBMCs from IDDM patients in response to 247-269 h6GAD65 peptide has been used to support the molecular mimicry model in which coxsackie B4 infection triggers a response from T cells that leads to IDDM (103). These T cells are then able to recognize previously non-immunogenic fragments of hGAD65.

iii) *Pre-proinsulin/Proinsulin/Insulin*

Insulin, secreted by pancreatic β-cells, is a 51 amino acid heterodimeric protein linked by two interchain cysteine bonds between a 21 amino acid A chain and a 30 amino acid B chain (Cys^{7}-Cys^{7}, Cys^{20}-Cys^{19}). A third intrachain disulfide bond is found in the N-terminal portion of the A chain, forming a loop structure (Cys6-Cys11). Insulin is derived from proinsulin, containing an additional 33 amino acid connecting-, or C-peptide

that links the A and B chains. Proinsulin is derived from cleavage of a 19 amino acid signal sequence from preproinsulin. Immune responses to proinsulin have thus far largely been represented only by circulating autoantibodies (89), although Rudy *et al* reported that residues 24-36 of proinsulin, which share marked similaity to amino acids 506-518 of GAD, elicit strong responses from T cells derived from patients predisposed to IDDM (121). Further, Chella David's group has made some progress in defining peptides of human proinsulin capable of eliciting T cell responses to residues 1-24 and 44-63 of preproinsulin (122).

Numerous reports of T lymphocyte responses to insulin (as opposed to proinsulin) and the epitopes involved have been made in both man and mice (123-126). Several groups have reported on the class II-restricted response of murine T hybridomas to the N-terminal portion of the insulin A chain, utilizing different sources of insulin. In one study, residues critical for MHC class II restriction and TCR recognition were mapped to residues 1-13 or 1-14 (124). These peptides were found to provide stimulation equivalent to the full A chain. However, truncation of the two most N-terminal residues from the 13-mer or 14-mer resulted in a 100-fold drop in T cell reactivity, possibly reflecting a deviation from ideal class II peptide length or a loss of critical residue for MHC or TCR recognition. A second group of T hybrids was shown to react to the full A chain but not the N-terminal 13- or 14-mer, suggesting the presence of a second epitope in the carboxy-terminal end of the A chain. No responses to the insulin B chain were noted.

Responses to human insulin by PBMCs from IDDM patients and related non-diabetic individuals were reported by Naquet *et al* (126). A T cell epitope, consisting of A(1-14)/B(1-16), was recognized by both diabetics and non-diabetics. Nearly all diabetics (5/6) and few related non-diabetics (2/6) had PBMCs that proliferated in response to the A(1-14) peptide. One-half of the diabetics tested and one non-diabetic could also respond to residues 10-25 of the B chain derived from beef insulin. Since beef insulin

B-chain differs from that of its human analogue only at residue 30, this region, along with A(1-14), were proposed to comprise the immunodominant epitopes of human insulin. However, responses in diabetics could be unrelated to the autoimmune response. Interestingly, the same group noted that the T cell response to human insulin was restricted by HLA-DR3, -DR4, and -DR5, as well as HLA-DQw2 and -DQw3.

iv) *BSA/ABBOS peptide/p69*

Epidemiological data has implicated bovine milk proteins, particularly BSA, in the onset of IDDM, noting the inverse correlation between breast-feeding and the frequency of IDDM (127). Early immunization of the BioBreeding (BB) rat, a rodent model for diabetes, with BSA was found to accelerate the onset of diabetes (128). Anti-BSA antibodies have been reported to bind an a 69kd β-cell surface protein, termed ICA69 (129, 130). The link between BSA or cow's milk proteins is postulated to be an environmental one based on molecular mimicry. This p69 protein has been demonstrated to be inducible by γ-INF (129, 131). A model was put forth suggesting that systemic release of γ-IFN by unrelated infectious events results in increased cell-surface expression of p69 and potential for triggering the autoimmune condition by virtue of circulating antibodies or T cells primed from previous encounters with BSA (132). This model may seem even more plausible in light of γ-IFN's demonstrated ability to induce class II expression in several cell types.

The connection between BSA, p69 and IDDM became stronger with the observation that a 17 amino acid stretch of BSA (residues 152-168), termed the ABBOS peptide, which differs from the sequence of human, mouse and rat albumins, could induce the formation of antibodies to ICA69 in BB rats immunized with the ABBOS peptide (19). 30he cDNA encoding rat and human p69 was cloned from a rat islet cell library, with the

human variant identified by cross-hybridization (133). The cloned p69 was shown to induce proliferation of T cells from diabetic children, but also from control children.

Animal Models of IDDM: Non-Obese Diabetic Mice

Research into the molecular mechanisms of IDDM have been confounded by the limitations posed by working with human subjects. Fortuitously, a mouse strain was discovered that spontaneously develops autoimmune diabetes. Disease has been associated with at least 14 different loci and while the NOD MHC is essential for incurring diabetes, it is not sufficient, implicating other non-MHC encoded factors in disease (134). Development of insulin dependent diabetes in NOD mice is preceded by insulitis, the progressive accumulation of lymphocytes within pancreatic islet cells. Within 3 to 7 months of birth, 80-90% of females and 40-50% of males have developed insulin dependence (135). While the extent to which NOD mice mimic human IDDM is debatable, NOD mice have facilitated the analysis of class II and T cell interactions in the disease process. Interestingly, the NOD class II I-A_{β}^{g7} chain encodes a change from aspartate at position 57 to serine similar to that found in the human DQB1*0302 molecule, lending support to the use of NOD mice as a model for IDDM and raising the question of whether these two molecules are infact presenting a similar peptide (136). NOD mice have been used to analyze T cell responses to a number of putative autoantigens, such as GAD and insulin.

Experimental Design

The objective of this thesis was twofold: to assess the usefulness of a novel reporter gene, green fluorescent protein (GFP), as an indicator of T cell activation, which could then be applied to the identification of environmental antigens that may be cross-reactive

with diabetic autoantigens, and to develop T cell hybridomas that could be used to define NOD-restricted, hGAD65 epitopes. Chapter 3 outlines the identification of T cell epitopes of hGAD65 in NOD mice. Chapter 4 describes the production and testing of a novel GFP-inducible T cell fusion partner.

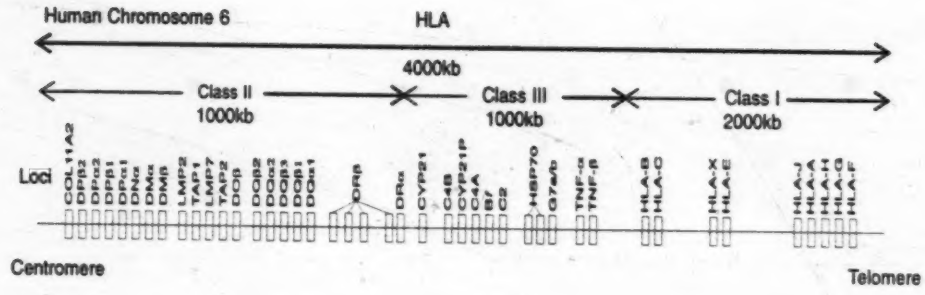

FIGURE 1.1. Schematic of Human Leukocyte Antigen Complex on chromosome 6

Chapter II

MATERIALS AND METHODS

1) PCR

PCR was performed using a PTC100 Programmable Thermal Controller (MJ Research Inc., Watertown, MA, U.S.A). A 50µl reaction was prepared in a Perkin-Elmer GenAmp tube (Perkin-Elmer, Foster City, California, USA) as follows: H_2O, template DNA (100ng human genomic DNA or 10ng plasmid DNA/cDNA), 5µl 10X PCR buffer (50mM KCl, 10mM Tris HCl pH 8.4, 200µg/ml gelatin), 1.0µM 5' and 3' primers each (Table 2.1), and 1.0-3.0mM $MgCl_2$. Tubes were heated at 80°C for 1 min prior to the addition of 5ul of a DNA polymerase enzyme mixture, consisting of 1µl (5 units) recombinant *Taq* DNA polymerase prepared in our laboratory and 0.1µl (0.2 units) Vent polymerase (New England Biolabs, Beverly, MA, U.S.A) for genomic DNA templates, or 1µl *Pfu* polymerase (Stratagene, La Jolla, CA, U.S.A.) for plasmid/cDNA templates. PCR was performed for 25 cycles according to standard methods with denaturation at 94°C for 15 seconds, primer annealing at 54-56°C for 30 sec, and extension at 72°C for appropriate time periods (typically 45-90sec). PCR products were analyzed on agarose gels (GIBCO BRL, Grand Island, N.Y., U.S.A.) made in TBE buffer (0.045 Tris-borate, 0.001M EDTA) and visualized on a 365nm U.V. transilluminator (UVP, San Gabriel, CA, U.S.A.).

PCR from cells was performed by washing $1x10^4$ cells twice with 1ml PBS in a microcentrifuge tube. Cells were resuspended in 50µl H_2O and placed in boiling water for

5min. Cellular debris was pelleted and the supernatant was added to 50µl of a 2X solution of PCR salts and PCR performed as described above.

2) Clean Up of PCR Products, Restriction Enzyme Digestion, and Ligation

Microcon 100 microconcentrators (DNA cutoff= 125b.p.; Amicon, Beverly, MA, U.S.A.) were used to remove primers and deoxynucleotides from successful PCR reactions. Microcons were pre-equilibrated with TE by adding 400ul TE to sample reservoir, centrifuging at 10,000 x*g* for 5min, and removing the dialysate from the lower tube. The contents of a larger PCR reaction (90µl) and TE (310µl) were added to the sample reservoir, the microcon centrifuged for 5min, and the dialysate removed from the lower tube. This dialysis procedure was repeated twice by filling the sample reservoir with TE to a final volume of 400µl and centrifuging for 5min on the second spin and 7min on the third spin. The duration of the final spin was increased to concentrate the DNA, which was subsequently recovered by a 10min reverse spin of the upper sample reservoir into a fresh microfuge tube.

DNA was prepared for subcloning by restriction enzyme digestion. Dialysed DNA was typically digested in a final volume of 22.5µl, according to manufacturer's directions for buffer choice, cutting duration and enzyme concentration.

4) beta-agarase digestion and ligation

Linearized plasmids or enzymatically digested PCR fragments were resolved by LMP-agarose (SeaPlaque GTG Agarose; FMC BioProducts, Rockland, ME, U.S.A.) electrophoresis using TAE buffer (0.04M Tris-acetate, 0.001M EDTA). DNA bands were visualized on a 365nm UV transilluminator to prevent DNA degradation and desired bands were excised with a scalpel into microcentrifuge tubes. Gel slices were pelleted in a microcentrifuge for 1min at 14,000rpm and one-tenth volumes-worth of beta agarase

digestion buffer (NEB) was added to the gel. Tubes were incubated at 70°C for 5min, removed and mixed by hand, and then replaced at 70°C for a further 5min. Samples were then equilibrated at 42°C for 10min followed by the addition of 1 unit of beta-agarase I enzyme (New England Biolabs). Samples were incubated at 42°C for 2hr, placed in ice for 10min to polymerize any undigested agarose and then spun at 16,000 x*g* for 10min. DNA-containing supernatant was transferred to a fresh tube and precipitated by addition of 0.7 volumes of isopropanol and incubation at -20°C for 1hr. DNA was pelleted by centrifugation at 14,000rpm for 30min at 4°C, washed with 70% EtOH, and resuspended in 20µl of TE.

DNA ligations were performed in a total volume of 20 µl. Appropriate amounts of linearized vector and insert were added to a microcentrifuge tube with 2 µl of 10X T4 DNA ligase buffer [500 mM Tris-HCl (pH 7.8), 100 mM $MgCl_2$, 100 mM DTT, 10 mM ATP, 250 µg/ml BSA] and 80 units of T4 DNA ligase (New England Biolabs). Samples were incubated at 16°C to promote efficient ligation.

3) **Transformation of *E.coli***

100 µl of transformation-competent DH5α cells were thawed on ice, to which was added 12 µl of an overnight ligation reaction. Tube contents were resuspended by hand and incubated on ice for 15min. Cells were then heat-shocked at 37°C for 90 seconds afterwhich 1ml of 2X YT/T medium (1.6% w/v bact-tryptone, 1% bact-yeast extract, 0.5% NaCl) was immediately added. Cells were outgrown at 37°C on a rollerdrum (New Brunswick Scientific Equipment, Edison, NJ, U.S.A.) at maximum speed. 100 µl of this cell suspension was used to plate out colonies on a LB plate (1%w/v bacto-tryptone, 0.5%

bacto-yeast extract, 1% NaCl) containing 100 µg/ml carbemicillin. Then remaining cells were pelleted in a microcentrifuge for 10 seconds at 16,000 x*g*, resuspended in a volume of 100 µl 2X YT/T , and plated out. Plates were incubated overnight at 37°C.

4) Plasmid DNA Preparation

Individual bacterial colonies were expanded in 2 ml of 2X YT/T supplemented with 100 µg/ml ampicillin overnight at 37^{0}C on a rollerdrum. 1 ml of cell suspension was pelleted in a microcentrifuge tube at 16,000 x*g* for 10 seconds and the supernatant discarded. Cells were first resuspended in 80 µl of resuspension buffer [50 mM Tris-HCl (pH 8.0), 10 mM EDTA, 100 µg/ml RNAseA] and then lysed at room temperature by addition of 100 µl of lysis buffer (200 mM NaOH, 1% SDS). 100 µl of ice-cold neutralization buffer [3 M KOAc (pH 5.5)] was added to refold plasmid DNA and samples were incubated on ice for 20 min. Cellular debris and precipitated genomic DNA was separated from plasmid DNA by centrifugation at 16,000 x*g* for 30 min at room temperature. Supernatants were transferred to fresh tubes and plasmid DNA precipitated with 250 µl of isopropanol. DNA was pelleted by centrifugation, washed with 70% EtOH, and resuspended in 50 µl of TE. Plasmids were mapped by restriction enzyme analysis and agarose gel electrophoresis using previously described techniques.

For preparation of large amounts of plasmid DNA, 150 ml of superbroth supplemented with 100 µg/ml of ampicillin was inoculated with plasmid-containing bacteria and grown overnight. Bacteria were pelleted at 15,000x*g*, resuspended in 4ml of buffer 1 [25 mM Tris-HCl (pH 8.0), 10 mM EDTA, 50 mM glucose], and transferred to Oakridge tubes (Nalgene, Rochester, NY, U.S.A.) . To this was added 1 ml of 25 mg/ml lysozyme in buffer 1. The sample was mixed and incubated on ice for 20 min. 10 ml of freshly made buffer 2 (0.2 N NaOH, 1% SDS) was added, samples mixed by inversion, and

incubated for 10min at room temperature to facilitate cell lysis. 10ml of buffer 3 [3 M KOAc (pH 5.5)] was added, samples mixed, and incubated on ice at 4^0C for 2 hours to refold plasmid DNA. Cellular debris was pelleted at 30,000x*g* for 30 min at room temperature, supernatant transferred to 50 ml polypropylene conical tubes (Becton Dickinson Labware, Franklin Lanes, NJ, U.S.A). Supernatants were supplemented with 2.5 µg of RNAse A (Boehringer Mannheim), incubated for 60 min at 37^0C, and then extracted with a 1:1 mixture of phenol:chloroform. The aqueous phase was removed, transferred to a polyallomer centrifuge tube (Beckman Instruments Inc., Palo Alto, CA, U.S.A.), precipitated with 0.7 volumes of isopropanol and incubated at -20^0C for one hour. DNA was pelleted by centrifugation in an SW28 rotor (Beckman Instruments Inc.) at 15,000rpm for 15 min. DNA was resuspended in 1.5 ml TE to which was added 3 ml of a CsCl stock solution (1.2 g/ml, reference index of 1.4155 visualized with a refractometer). This solution was transferred to a polyallomer Quick-Seal centrifuge tube (13x51 mm, Beckman Instruments Inc.) and 100 µl of a 100 mg/ml solution of EtBr added. The tube was filled with a CsCl:H_2O (2:1) solution, sealed, and centrifuged overnight at 55,000rpm at 19^0C.

Banded plasmid DNA was removed from the tube using an 18G needle attached to a 3 ml syringe. EtBr was extracted five times using an equal volume of water-saturated butanol and the remaining aqueous solution brought to a volume of 6.3ml in a 14 ml polypropylene snapcap tube (Falcon 2059, Becton Dickinson Labware). 700 µl of a 3 M NaOAc (pH 7.4) solution was added followed by 5 ml of isopropanol. The solution was incubated at -20^0C for one hour and then centrifuged at 3000x*g* to pellet DNA. DNA was precipitated once again using EtOH, washed in 70% EtOH and resuspended in TE.

5) Cell Culture

BW α−β−, murine T cell hybridoma cell lines,murine lymph node cells, and transfected BW α−β− were cultured in RPMI 1640 (GIBCO BRL, Grand Island, N.Y., U.S.A.) supplemented with 10% (v/v) Fetal Clone I (HyClone, Logan, Utah, U.S.A.), 1mM L-glutamine (GIBCO BRL, Grand Island, N.Y., U.S.A.), and 0.01 M 2-mercaptoethanol. Murine lymph node cells were initially isolated in HBSS to prevent osmotic shock. All cells were cultured in a humidified, 5% CO_2 incubator.

6) Immunization of Mice

Antigen suspensions were prepared by vortexing a 1:1 mixture of a 1mg/ml PBS-dissolved antigen solution:CFA (GIBCO BRL, Grand Island, N.Y., U.S.A.) in a 1 ml tuberculin syringe for 15 min at maximum speed. Mice were immunized in the rear footpad with 25 µg (50 µl) of the antigen suspension. Seven days later, mice were boosted in the same footpad with 25 µg (50 µl) of a similar suspension, made with IFA.

7) Isolation and Culture of Lymph Node Cells

Mice were sacrificed by cervical dislocation seven days after being boosted with antigen. The draining popliteal lymph node was removed by dissection and placed into 10ml of cold HBSS supplemented with 100 units each of penicillin and streptomycin. Lymph node cells were obtained by maceration of lymph nodes between frosted ends of frosted microscope slides. Suspensions were layered on to 3 ml of Lympholyte-M (Cedarlane, Ontario, Canada) and centrifuged at 1500 x*g* for 20 min. Lymphocytes were collected from the inteface, washed with 10 ml of RPMI. Isolated lymph node cells were cultured with the appropriate amount of antigen in enriched RPMI at a concentration of 4 x

10^6 cells/ml for 48 hrs.

8) T cell Hybridoma Production

All manipulations were performed with reagents at 37°C. As well, RPMI without HEPES was used due to the cytotoxicity associated with co-exposure of cells to both HEPES and PEG. IL-2 stimulated cells were collected by centrifugation over Lympholyte-M as before, and cultured for a further 48 hrs with 50 units/ml recombinant murine IL-2. Cells were then collected by centrifugation over Lympholyte-M, washed with RPMI (without HEPES), and counted in a hemacytometer. Note that all cells involved in the fusion were not exposed to HEPES to prevent HEPES-mediated cell toxicity upon exposure to PEG.

Lymph node cells were then combined in a 50 ml conical tube with an equal number of BW α–β– or $NFAT_3$-GFP-transfected BW α–β– fusion partners that had been washed three times by centrifugation at 200x*g* with 37°C serum- and HEPES-free RPMI. In between washes, RPMI was kept in a 37°C waterbath. After the final wash, the tube was placed in a 250 ml beaker containing 37°C H_20 and over the course of 1 minute, 1 ml of 37°C PEG was added dropwise with gentle swirling of the tube. The PEG was immediately diluted out with gentle swirling using 37°C RPMI as follows: 1 ml over the first 30 sec, 2 ml over the next 30 sec, 3 ml over the next 30 sec, and then 4 ml over the next 30 sec. The tube was then incubated in a 37°C water bath until the total exposure to PEG had reached 8 min. Forty ml of RPMI was then added slowly, the tube inverted gently three times, and the cells then pelleted at 200x*g* for 5 min. Cells were resuspended

gently with 37°C enriched RPMI supplemented with hypoxanthine-azaserine ($1x10^{-5}$ M and $5.78x10^{-6}$ M, respectively) at $2.5x10^5$ cells/ml and 100 µl was plated out per well into 96 well flat-bottomed plates (Becton Dickinson Labware) and incubated at 37°C. Clones were picked and expanded as they came up (typically after 14 days).

9) T cell Stimulation

i) antigen presentation assays:

T cell antigen specificity was analyzed by incubation of 1×10^5 T hybrid cells with 2×10^5 syngeneic splenocytes irradiated with 2000rads. Cells were incubated in a volume of 200 µl with the appropriate amount of protein or peptide antigen in triplicate for 24 hours, after which culture supernatants were analyzed by ELISA for the production of IL-2.

ii) PMA/ionomycin:

1×10^5 T lymphocytes were cultured in the presence of 10ng/ml PMA and 100 µM ionomycin for a period of 24 hours in 96 well plates in a volume of 200µl.

iii) anti-CD3

96 well plates (CoStar, Cambridge, MA, U.S.A) were coated overnight at 4^0C or for one hour at 37^0C with 100 µl of a 1 µg/ml solution of the H57-597 antibody dissolved in PBS. Plates were washed three times with 200 µl of PBS and 1×10^5 were then added in a volume of 200 µl of enriched RPMI. Cells were incubated for 24 hours at which point cells and/or supernatant were collected for analysis.

10) **IL-2 ELISA**

96 well enzyme immunoassay plates (EIA/RIA Plates #3590, CoStar, Cambridge, MA, U.S.A.) were coated overnight at 4^0C or for 30 min at room temperature with 100 µl of a 1 µg/ml solution of rat anti-mouse IL-2 antibody (clone JES6-1A12; Pharmingen, San Diego, CA, U.S.A.) dissolved in PBS. Plates were washed three times with PBST. 75 µl of T cell culture supernatants were captured for 30 min at room temperature. Purified, recombinant murine IL-2 (Pharmingen) was used to establish a standard curve, ranging from 175 to 0.171 U/ml in two-fold, serial dilutions. Wells were washed 3 times with PBST, 100 µl of a 1 µg/ml solution of biotinylated rat anti-mouse IL-2 (clone JES6-5H4, Pharmingen) in 1% BSA/PBST was added, and plates were incubated for 30 min at room temperature. Plates were washed three times with PBST, and 75 µl of a 1:5000 solution of streptavidin-HRP (Jackson ImmunoResearch Laboratories Inc., West Grove, PA, U.S.A.) prepared in 1% BSA/PBST was added for 30 min at room temperature. Plates were washed five times with PBST, 100 µl of an ABTS developing solution added, and the developing reaction allowed to proceed for 20 min in the dark at room temperature. Plates were read in a multiwell spectrophotomoter (Molecular Devices,) using a 405nm filter with a 490nm background subtraction.

11) **FACScan/FACSort**

All procedures were performed on ice. 1 x 10^5 T cells were collected in 4.5ml capless, conical tubes (Sarstedt, Germany) and pelleted at 200 x*g*. Cells were washed with ice-cold SM (HBSS, 5% FCS, 1mM EDTA), resuspended in 200 µl of ice-cold SM supplemented with a 1:100 dilution of appropriate FITC-conjugated antibody, and incubated for 20 min on the dark. Cells were then underlayed with 1 ml of FCS, pelleted at

200 x*g* and then resuspended in 200 µl of ice-cold SM. Cells were analyzed using a FACScan system (Becton Dickinson).

12) **Electroporation of Plasmid DNA**

1 x 10^7 BW cells were washed twice with 30ml of ice cold HBS, resuspended in 400 µl of HBS, and transferred to an ice-cold 0.4 cm gap electroporation cuvette (BioRad, Mississagua, ON, Canada) along with 400 µl of linearized DNA (200 µg of each plasmid bearing a gene of interest in addition oto 10 µg of drug-resistance encoding plasmid pSSD5.neo) suspended in HBS and placed on ice. Cells were electroporated at 200volts, 960µF, immediately returned to ice for a period of 5 min, and then transferred to a culture flask containing 37°C enriched medium supplemented with 100 U each of penicillin and streptomycin. After 24 hrs of culture, cells were plated out at 2 x 10^4 cells/well in 48-well plates in the presence of 600 µg/ml geneticin. Individual clones were then tested for protein inducibility.

13. **Propidium Iodide Staining of T cells**

T cells were transferred to 15ml polypropylene culture tubes and pelleted at 100 x*g*. Cell pellets were washed once in ice-cold PBS and then resuspended in 0.5-1.0ml PBS. 0.5-1.0mlof heat-inactivated fetal calf serum was added. Cells were gently agitated on a vortex while 3ml of ice cold 70% EtOH was added down the wall of the centrifuge tube, afterwhich the tube was closed and inverted gently once to ensure complete mixing. Cells were incubated on ice for 30min, pelleted by centrifugation, and washed once with 1-2ml PBS. Cells were resuspended in 0.5-1mlof 50µg/ml PI in PBS and placed on ice for at least 10-20min before detection by FACS.

TABLE 2.1. Oligonucleotides used in the course of cloning.

Primer Name	Primer Sequence* (5'→3')
5'IL-2 (Hind III)	**AAGCTT**TTCTCTAGCTGACATGTAAGAA
3'IL-2	**CTCGAG**TTGAGGTTACTGTGAGTAG
NFAT 114 (Hind III)/(Pst I)	CTCTCT**AAGCTT**GGAGGAAAAACTGTTTCATACAGAAG GCGTGGAGGAAAAACTGTTTCATACAGAAGGCGTGGAG GAAAAACTGTTTCATACAGAAGGCGT**CTGCAG**CTCTCT
5'NFAT 114 (Hind III)	CTCTCT**AAGCTT**GGAGGAAAA
3'NFAT 114 (Pst I)	CTCTCT**CTGCAG**ACGCCT
5'IL2(-70) (Pst I)	CTCTCT**CTGCAG**CATTTTGACACCCCCCATAATAT
5' GFP (Mlu I)	**ACGGCT**ATGAGTAAAGGAGAAGAACTTTT
3'GFP (Not I)	**GCGGCCGCT**ATTATTTGTATAGTTCATCCATGC

*PCR primers used in the course of cloning. Primers were syntehsized on an Applied Biosystems Model 391 PCR-Mate DNA Synthesizer. Restriction sites indicated in brackets after teh oligonucleotide's name are highlighted in bold in the corresponding sequence.

Chapter III

CHARACTERIZATION OF NOD-RESTRICTED T CELL EPITOPES TO HUMAN GLUTAMIC ACID DECARBOXYLASE 65 USING T CELL HYBRIDOMAS

Introduction

The identification of T cell epitopes for a particular autoantigen can be done several ways. The first involves studying the binding of individual peptides (from an overlapping set) to the purified class II molecule of interest. Binding affinity does not necessarily correlate with peptide immunogenicity as has been demonstrated for the immunodominant, EAE-inducing myelin basic protein peptide (Ac1-11) which has been shown to bind with weak affinity to its class II I-A^u restricting element (137). This mechanism has also been suggested to exist for the NOD class II I-A_β^{g7} molecule, which has been suggested to form an unstable complex with peptides based on electrophoretic analysis of the class II molecule in the presence of SDS (138). T cell epitopes can also be analyzed by immunizing mice with either whole antigen or with individual peptides that encompass the whole antigen. The drawback of the latter immunogen is that it is not clear whether APCs would process and present the same peptides that are arbitrarily made, establishing the use of whole antigen immunizations and reliance upon APCs to present the correct epitopes in vivo as the preferred strategy.

These approaches and others have been used to delineate T cell epitopes to both human and murine GAD in NOD mice. The importance of T cell responses to hGAD65 in mice is evident from studies in which intrathymic injection of hGAD65 into 4wk old female NOD mice was found to prevent diabetes (139). The first published study of T cell epitopes

to human GAD found that GAD was the first beta-cell antigen to which T cells responded and that this response correlated well with the onset of insulitis (140). The incubation of splenocytes from unprimed 4 week old NOD mice with an overlapping set of hGAD65 peptides was used to demonstrate that responses could initially be elicited against two adjacent regions of the protein: amino acids (aa) 509-528 and aa524-543. Within the next three weeks, reactivity spread to several regions of the protein, including aa 246-66, which shares a six residue consensus with the coxsackie P2-C protein. This lends support to the molecular mimicry hypothesis. It should be noted that this approach to mapping epitopes in hGAD65 could conceivably overlook hGAD65 epitopes localized to regions of non-homology between hGAD65 and murine GAD 67, which is the predominant form of GAD in mouse islets (141).

Studies to assess the impact that *in vivo* antigen processing has on the generation and recognition of hGAD65 epitopes in NOD have only recently been performed. Chao *et al* have identified four NOD-restricted hGAD65 T cell epitopes by immunization of mice with whole protein and screening T cell hybridomas with overlapping peptides. Four epitopes were identified: aa206-220, 221-235, 286-300, and 571-585. (142). Zechel *et al* identified three additional epitopes corresponding to aa 78-97, 202-221, and 217-236 (143). Interestingly, these groups did not identify any of the previous 'epitopes' identified in the original report of NOD-restricted hGAD65 epitopes identified in unprimed mice. This underscores the potential importance of in vivo antigen processing and display of naturally-processed epitopes, and also possible differences between epitopes associated with the autoimmune process versus the epitopes obtained by classical recall responses from unimmunized mice (140) or mice immunized with peptides.

This study focused on the development of T cell hybridomas from NOD mice that could be used to map epitopes in human GAD-65. The results are presented below.

Results and Discussion

Female NOD mice were immunized with recombinant human GAD-65 produced in our laboratory which encoded aa 90-585 of the GAD protein (144). This deletion of the N-terminus was necessary to achieve protein production in E. coli, since the full length protein was highly toxic. Draining lymph node cells were stimulated with antigen and then expanded in IL-2 to increase the number of antigen specific cells that would be fused. A variety of different stimulation and expansion protocols are used by different groups. In this study, draining lymph node cells were stimulated with antigen for a period of 48hrs, based on studies of antigen-stimulated T cells that showed IL-2 receptor expression peaked 48hrs post-activation (145). Cells were then expanded in recombinant IL-2 for another 48hrs based on empirical observations that this time frame resulted in the greatest expansion and/or recovery of cells.

Following fusion, cells were plated out immediately into 96 well plates (288 wells in total) in hypoxanthine-azaserine, as opposed to the traditional hypoxanthine-aminopterin-thymidine selection agent. Azaserine has been reported to result in faster hybrid growth rate, as well as enhanced hybrid stability (146). Twenty-one of 119 resulting hybridomas were immediately tested for antigen specificity as described in Materials and Methods. At this point it should be noted that developing hybridomas may be tested for expression of TCR first, as opposed to antigen specificity; this allows one to only test those hybridomas that express appreciable levels of TCR. We chose to proceed immediately to testing specificity to expedite the recovery of a specific T hybridomas and to minimize the impact that chromosome stabilization would have on recovery of an antigen-specific clone. Five hGAD65-reactive lines (NG 1, 2, 17, 18, 25; Table 3.1) were identified and then single cell cloned into 96 well plates using a Coulter Epics Elite FACS machine and the Autoclone program. Only 33 clones from the two parental lines which produced the highest amount of IL-2 upon exposure to antigen (NG 17 and NG 18) were re-evaluated for antigen

specificity due to limited antigen availability, yielding 26 lines that produced significant amounts of IL-2 relative to controls (Table 3.1). Only clones NG 17.5 and NG 18.13 were then tested against a panel of overlapping peptides encompassing the entire hGAD-65 protein (Chiron, Clayton, Victoria, Australia; Table 3.2). Clone NG 17.5 was found to respond strongly to peptide 56 of the overlapping set, corresponding to aa551-570 of hGAD65 (Table 3.3). NG 17.5's response to whole GAD has significantly from the initial results presented in Table 3.1; this may reflect a decrease in TCR expression levels, which may be confirmed by TCR staining. NG 17.5 produced a very large amount of IL-2 in response to the $hGAD65_{551-570}$ peptide, which likely reflects the increased molar concentration of the epitope provided in peptide form as compared to that which APCs must generate provided with the entire protein.

Conclusions

A protocol to produce murine T cell hybridomas has been established and used to identify T cell epitopes of hGAD65. Two T cell hybridomas of different lineages were tested for their reactivity to an overlapping set of peptides of hGAD65 and one of these clones, NG 17.5, was found to react to a previously unreported hGAD65 T cell epitope, aa551-570. Wicker *et al* have actually reported that amongst an overlapping set of peptides to hGAD65, $hGAD65_{551-570}$ exhibits the highest binding affinity to another human class II molecule found associated with with IDDM in Caucasians, HLA-DRB1*0401 (144, 147), while $hGAD65_{551-570}$ was found to bind weakly to purified HLA-DQ8. In the same study, DRB1*0401-transgenic mice immunized with $hGAD65_{554-566}$ mounted strong responses upon in vitro antigen recall. Another study demonstrated that of fourteen T cell hybridomas produced from hGAD65-immunized DRB1*0401-transgenic mice, all responded to aa551-565 (148). Thus, the core T cell epitope recognized within $hGAD65_{551-570}$ may reside

within the first fifteen residues. As with the reports of NOD-restricted hGAD65 T cell epitopes by Chao *et al* (142) and Zechel *et al* (143), these studies emphasize the importance of in vivo antigen processing in delineating T cell epitopes. Thus, in order to investigate the role, if any, of $hGAD65_{551-570}$ in diabetogenesis, studies of hGAD65 epitopes in HLA-DQ8 transgenic mice are critical.

The $hGAD65_{551-570}$ epitope can also be considered in the context of a model $I\text{-}A_\beta^{g7}$-peptide binding motif put forth by Harrison *et al* based on the analysis of binding of a known $I\text{-}A_\beta^{g7}$-restricted hen egg lysozyme T cell epitope, HEL_{9-27}(149). Utilizing amino acid substitution analysis, they defined a minimal 10aa sequence (HEL_{12-21}) within this peptide that was required for T cell activation and a 9aa core sequence (HEL_{13-21}) critical to binding to purified $I\text{-}A_\beta^{g7}$. Within this core sequence, they defined a peptide binding motif located at position 6 and 9 relative to the original HEL_{12-21} core epitope that is postulated to anchor the peptide to the class II binding groove. The first anchor residue optimally encoded a large, hydrophobic residue (leucine, isoleucine, valine, or methionine) a second residue, two to three residues from the first, favoured aromatic and hydrophobic (tyrosine or phenylalanine) or positively-charged residues (lysine, arginine). When they compared sequences of 30 peptides known to bind to $I\text{-}A_\beta^{g7}$, 27 peptides were found to incorporate one or both elements of this motif into their structure. Notably, this motif was found associated with the three hGAD65 epitopes previously described by Kaufman *et al* (Table 3.4) (140). They also note that binding assays using purified class II molecules and peptide analogs is more accurate in defining a peptide binding motif since compared to other methods such as elution of bound peptides from purified class II and alanine or other scans to known epitopes tested for presentation to T cells. This makes sense as both of these methods are limited to qualitative assessments of peptide motifs that do not directly

address quantitative aspects of peptide binding. This is reflected in Quinn *et al*'s report on putative I-A_{β}^{g7} contact residues in the hGAD65 aa524-543 peptide (150). Truncated peptides and their effects on activation of T cell hybridomas raised to the nominal peptide were used to establish a core immunogenic peptide corresponding to aa527-538. Amino acid substitutions were used to identify four putative MHC contact residues: 530 (alanine), 531 (proline), 536 (arginine), and 537 (methionine). In comparing the peptide motifs thus defined by Harrison and Quinn, different methods have yielded different anchor residues; infact, Quinn's minimal peptide sequence excludes the motif defined by Harrison for the same peptide on the same class II MHC. However, upon closer examination, Harrison's motif can be localized to aa533 (isoleucine: large, hydrophobic) and aa536 (arginine: positively charged) within the core aa527-538 hGAD65 peptide. In contrast, only one of the four novel epitopes reported by Chao and two of three reported by Zechel are found to incorporate this peptide binding motif. The peptide identified in this project, aa551-570, appears to support this peptide-binding motif, as it displays a similar arrangement of a large hydrophobic residue ($valine_{554}$) separated by two residues from an aromatic and hydrophobic amino acid ($phenylalanine_{557}$). These reults are summarized in Table 3.4.

A comparison of the $hGAD65_{551-570}$ epitope to its corresponding regions in the mouse GAD proteins (mGAD65 and mGAD67) demonstrates complete sequence identity with a twenty amino acid sequence in the smaller isoform and 80% sequence identity with its cognate region in the larger, 67kD isoform (Figure 3.1). In NOD mice, mGAD67 is thought to play a pivotal role in diabetogenesis (109, 110) . Thus, it may be that the differences in the hGAD65 epitope may be sufficiently different from the self-derived protein so as to elicit an immune response. This line of reasoning is supported by the fact that the difference in the fourth amino acid of this epitope, $alanine_{562}$ in mGAD67 and

valine$_{554}$ in hGAD65, helps to establish the I-A$_{\beta}^{g7}$ peptide-binding motif in the hGAD65$_{551\text{-}570}$ epitope. Thus, this epitope may be xenogeneic in nature.

Finally, a scan of the Swiss-Prot and PIR protein databases using the Basic Local Alignment Search Tool algorithm did not reveal any sequence identity between the hGAD65$_{551\text{-}570}$ epitope and any other protein in the databases, except for GAD proteins from other species. It may be that a protein which serves as tan autoimmune trigger in NOD mice remains to be characterized or that there is infact an alternative, non-infection-based environmental trigger, such as stress, that elicits disease.

Future Directions

While a successful T cell fusion protocol was worked out in the course of this project, there is room for improvement in the procedure. Future fusions may make use of FACSorting of specific, antigen activated T cells during the in vitro culture of draining lymph node cells based on expression of the IL-2 receptor, or CD25. This procedure has been used successfully before to isolate HLA-DQ8 restricted human T cell clones and may help to increase the antigen specific precursor frequency prior to IL-2 expansion (151). Furthermore, as T cell hybridomas are notoriously unstable cells, it may be worthwhile to 'capture' the TCR specificity by cloning the TCR cDNA's for any antigen specific clone that will be used in future experiments. This approach has been made possible by isolation of a spontaneous TCR-loss mutant of another hybridoma, 58α-β-, originally specific for an OVA-derived peptide (152). Cloning of the Vα and Vβ-regions of a desired TCR into vectors containing the murine Cα and Cβ sequences and co-transfecting these constructs into 58α-β- along with CD3ζ chain cDNA has been shown to restore antigen reactivity according to the specificity of the transfected TCR (153). While this strategy is time

consuming, it needs to be balanced between the inherent instability of T cell hybridomas and the importance of the hybridoma(s) to subsequent studies.

hGAD65-specific T cell hybridomas in NOD mice have been produced that react with a specific epitope of hGAD65. Having identified the epiopte specificity, future work with these hybridomas could perhaps focus on the early aspects of diabetogenesis, as T hybridomas can be experimentally considered to parallel thymocyte selection processes, as engagement of TCR/CD3 alone is sufficient to induce death in these cells.

TABLE 3.1. IL-2 produced by NOD-restricted, hGAD65-specific T cell hybridoma lines and daughter clones.*

T cell line/*clones*	Il-2 Produced (Units/ml)
NG-1	2.2
NG-2	1.2
NG-17	25.8
NG-18	11.1
NG-25	10.9
NG-17.5	49.1
NG-18.13	57.6

*T cells ($1x10^5$)were incubated with NOD splenocyte APCs ($2x10^5$) and 40μg/ml hGAD65 for 24 hrs in a volume of 200μl. Culture supernatants (75μl)were assayed for IL-2 by ELISA, as described in Materials and Methods. Negative controls consisting of T hybridoma cells incubated with APCs alone did not produce IL-2 beyond assay background levels.

TABLE 3,2. Sequences of overlapping peptides to hGAD65.*

Peptide	Sequence	Peptide	Sequence
1	MASPGSGFWSFGSEDGSGDS	30	ALGIGTDSVILIKCDERGKM
2	FGSEDGSGDENPGTARAWC	31	LIKCDERGKMIPSDLERRIL
3	ENPGTARAWCQVAQKFTGGI	32	IPSDLERRILEAKQKGFVPF
4	QVAQKFTGGIGNKLCALLYG	33	EAKQKGFVPFLVSATAGTTV
5	GNKLCALLYGDAEKPAESGG	34	LVSATAGTTVYGAFDPLLAV
6	DAEKPAESGGSQPPRAAARK	35	YGAFDPLLAVADICKKYKIW
7	SQPPRAAARKAACACDQKPC	36	ADICKKYKIWMHVDAAWGGG
8	AACACDQKPCSCSKVDVNYA	37	MHVDAAWGGGLLMSRKHKWK
9	SCSKVDVNYAFLHATDLLPA	38	LLMSRKHKWKLSGVERANSV
10	FLHATDLLPACDGERPTLAF	39	LSGVERANSVTWNPHKMMGV
11	CDGERPTLAFLQDVMNILLQ	40	TWNPHKMMGVPLQCSALLVR
12	LQDVMNILLQYVVKSFDRST	41	PLQCSALLVREEGLMQNCNQ
13	YVVKSFDRSTKVIDFHYPNE	42	EEGLMQNCNQMHASYLFQQD
14	KVIDFHYPNELLQEYNWELA	43	MHASYLFQQDKHYDLSYDTG
15	LLQEYNWELADQPQNLEEIL	44	KHYDLSYDTGDKALQCGRHV
16	DQPQNLEEILMHCQTTLKYA	45	DKALQCGRHVDVFKLWLMWR
17	MHCQTTLKYAIKTGHPRYFN	46	DVFKLWLMWRAKGTTGFEAH
18	IKTGHPRYFNQLSTGLDMVG	47	AKGTTGFEAHVDKCLELAEY
19	QLSTGLDMVGLAADWLTSTA	48	VDKCLELAEYLYNIIKNREG
20	LAADWLTSTANTNMFTYEIA	49	LYNIIKNREGYEMVFDGKPQ
21	NTNMFTYEIAPVFVLLEYVT	50	YEMVFDGKPQHTNVCFWYIP
22	PVFVLLEYVTLKKMREIIGW	51	HTNVCFWYIPPSLRTLEDNE
23	LKKMREIIGWPGGSGDGIFS	52	PSLRTLEDNEERMSRLSKVA
24	PGGSGDGIFSPGGAISNMYA	53	ERMSRLSKVAPVIKARMMEY
25	PGGAISNMYAMMIARFKMFP	54	PVIKARMMEYGTTMVSYQPL
26	MMIARFKMFPEVKEKGMAAL	55	GTTMVSYQPLGDKVNFFRMV
27	EVKEKGMAALPRLIAFTSEH	56	GDKVNFFRMVISNPAATHQD
28	PRLIAFTSEHSHFSLKKGAA	57	ISNPAATHQDIDFLIEEIER
29	SHFSLKKGAAALGIGTDSVI	58	ATHQDIDFLIEEIERLGQDL

*An overlapping set of 58 peptides to hGD-65 20aa in length with 10aa ovverlap, was synthesized commercially (Chiron) by conventional Fmoc chemistry using pin technology. Peptides were reconstituted to a stock concentration of approximately 200μg/ml in PBS and used at a concentration of 20μg/ml.

TABLE 3.3. IL-2 produced by NG 17.5 recognition of $hGAD65_{551-570}$.*

Antigen	Il-2 Produced (Units/ml)
hGAD 65	17.3
$hGAD65_{551-570}$	94.3

*T cells ($1x10^5$)were incubated with NOD splenocyte APCs ($2x10^5$) and either 40μg/ml hGAD65 or 20μg/ml of the $hGAD65_{551-570}$ peptide for 24 hrs in a volume of 200μl. Culture supernatants (75μl)were assayed for IL-2 by ELISA, as described in Materials and Methods. Negative controls consisting of T hybridoma cells incubated with APCs alone did not produce IL-2 beyond assay background levels.

TABLE 3.4. Presence of a defined I-A_β^{g7} peptide-binding motif within NOD-restricted, hGAD65 T cell epitopes.

hGAD65 Epitope	Peptide Sequence*	Presence of I-A_β^{g7}-binding motif	Reference
247-266	NMYAM**M**IAR**F**KMFPEVKEKG	+	140
509-528	IPPSLRY**L**LD**N**EERMSRLSK	+	
524-543	SRLSKVAPVIKAR**M**ME**Y**GTT	+	
206-220	TYEIAPVFV**L**LE**Y**VT	+	142
221-235	LKKMREIIGWPGGSG	-	
286-300	KKGAAALGIGTDSVI	-	
571-585	IDFLIEEIERLGQDL	-	
78-97	KPCSCSKVDVNYAFLHATDL	-	143
202-221	TNMFTYEIAPVFV**L**LE**Y**VTL	+	
217-236	EY**V**TL**K**KMREIIGWPGGSGD	+	
551-570	GDK**V**NF**F**RMVISNPAATHQD	+	-

*Amino acids that contribute to the presence of an I-A_β^{g7} peptide-binding motif within peptides are indicated in larger case, bolded letters. Weakly tolerated residues are underlined (149).

a)

```
hGAD65551-570:   551 GDKVNFFRMVISNPAATHQD 570
                     GDKVNFFRMVISNPAATHQD
mGAD65:          551 GDKVNFFRMVISNPAATHQD 570
```

b)

```
hGAD65551-570:   551 GDKVNFFRMVISNPAATHQD 570
                     GDK NFFRMVISNPAA+  D
mGAD67:          559 GDKANFFRMVISNPAASQSD 578
```

FIGURE 3.1. Comparison of sequence identity between $hGAD65_{551-570}$ and its corresponding sequence in mGAD65 and mGAD67. A gap fit was performed with the GCG Wisconsin Package, Version 8.1, UNIX 1995, to compare the $hGAD65_{551-570}$ sequence to the two murine GAD isoforms: **a)** mGAD65 and **b)** mGAD67.

Chapter IV

THE USE OF GFP COUPLED TO A MINIMAL IL-2 PROMOTER/ENHANCER TO STUDY T CELL ACTIVATION

Introduction

Molecular mimicry provides a credible and attractive explanation as to why particular individuals are susceptible to autoimmune diseases. Associations between both food and viral factors have been highlighted for IDDM. Analysis of mimicking epitopes in IDDM has relied first on the characterization of diabetogenic T cells that respond to a particular autoantigen by identifying the nominal peptide sequence that it recognizes, followed by a scan of protein databases to identify stretches of proteins that contain homologous sequences. While this approach identifies cross-reactive epitopes that can trigger a T cell, it does not address the ability of a T cell specific for an environmental antigen to elicit autoimmune disease. Thus, if T cell lines or clones could be raised in response to environmental antigens, they could then be tested for their ability to not only respond to autaoantigens in vitro, but to trigger autoimmunity in animals by adoptive transfer in animal models of disease. However, the low frequency of such cells confounds their isolation and analysis.

Sanderson *et al* have attempted to address this by exploiting the importance of the NFAT DNA element from the human IL-2 gene enhancer in T cell activation (154). NFAT, which is found only in activated lymphoid cells, is closely correlated with T cell activation and is strongly induced within 20 min of T cell stimulation, preceding IL-2 gene transcription by 20 min (155). Based on previous work (156), Sanderson *et al* produced a

novel T cell fusion partner that relies on three tandem copies of the human NFAT DNA binding sequence linked to a minimal IL-2 promoter to drive expression of bacterial beta-galactosidase (lacZ) (Figure 4.1). Hybridomas produced by fusion with this cell line would upon stimulation be expected to produce lacZ, and by incubating with the appropriate substrate (either fluorescent or colorimetric) would develop a spectrophotometrically-detectable product. This was confirmed upon fusion of a defined, antigen specific T cell clone with this fusion partner. Such a system, while offering an efficient method to assay T cell activation, relies on osmotic shock to load substrate into T cells and raises questions as to its suitably in the detection and recovery of live cells from animals for subsequent studies.

The goal of this project was to assess the use of an alternative reporter gene, green fluorescent protein, as both a general marker of T cell activation and as a molecular "tag" in specifically isolating those T cells that respond to environmental antigens within animal models of disease. GFP is responsible for the green portion of the bluish-green fluorescence emitted from the umbrella of the jellyfish, *Aequorea victoria* (157). This fluorescence is due to interaction of two proteins: aequorin and GFP. A portion of Aequorin, which is a complex of apoaequorin, an imidazolic coelenterazine, and molecular oxygen, is oxidized in the presence of calcium to produce blue fluorescent protein (BFP). In the presence of GFP, an energy transfer occurs from BFP to GFP, resulting in the jellyfish's fluorescent qualities (Figure 4.2) (158). The gene for GFP has been cloned and encodes a 238 amino acid, 27 kD protein. Fluorescence is due to post-translational modification of a hexapeptide sequence that generates a chromophore containing a cyclicized serine-dehydro-tyrosine-glycine trimer (159). GFP exhibits maximal blue light absorption at 395 with a minor peak at 470nm and emits green light maximally at 509nm with a minor shoulder at 540nm (160). The chromophore responsible for GFP's spectral qualities is able to withstand a number of harsh conditions, including heat, extreme pH,

and chemical denaturants (161). Although fluorescence may be lost upon exposure to base, acid, or denaturant, stabilization of pH and removal of the denaturant will allow for protein refolding and a return in fluorescence to previous levels. Expression of the GFP cDNA alone in bacteria, followed by excitation with blue light, yielded the characteristic green fluorescence of GFP in spite of the absence of additional gene products from *Aequorea victoria*, demonstrating the potential of GFP as a reporter gene (162). Successful expression of GFP under the control of the chicken beta-actin promoter and CMV enhancer sequence in mice with comparable levels of founder lines amongst mice injected with GFP or control human CD4 DNA illustrated GFP's sensitivity and lack of toxicity in vivo (163). Since then, GFP has been expressed in a number of cells and tissues of different organisms, both in vitro and in vivo. Most importantly, GFP's usefulness as a reporter is underscored by the fact that it does not require any sort of extraction procedure, as for chloramphenicol acetyltransferase, nor does it depend on enzymatic conversion of substrate to a detectable chromogen, as for luciferase and lacZ. Since no exogenously added substrates are required, GFP is more suitable for the study of living tissue and cells, especially if they need to be recovered for future experiments.

The cDNA sequence for GFP was cloned into an expression vector that utilized a tandem repeat of three NFAT binding sequences linked to a minimal IL-2 promoter to drive the reporter gene's expression. A positive control consisting of a portion of the 5' upstream region of the human IL-2 gene was linked to the same minimal IL-2 promoter and GFP cDNA. A novel fusion partner was produced by stable transfection of these constructs into the TCR-negative variant of the BW cell line and GFP inducibility was assessed by antigen-independent stimulation followed by fluorescent-activated cell sorting (FACS). Positive transfectants were single cell cloned and re-examined for inducibility. In order to assess the construct's antigen-specific inducibility, a single cell cloned transfectant was chosen for fusion with T cells from NOD-mice immunized with chicken egg

ovalbumin (OVA). Antigen-specific T cell hybridomas were then tested for GFP-inducibility.

Results and Discussion

The polymerase chain reaction (PCR) was used to amplify a 589 bp portion of the human IL2 promoter region from human genomic DNA, corresponding to bases -538 to +46, relative to the transcriptional start site. This amount of DNA was chosen so as to ensure that the necessary regulatory and enhancing elements would be present. Hind III and Xho I sites were incorporated into the 5' (AAGCTTTTCTCTAGCTGACATGT AAGAA) and 3' (CTCGAGTTGAGGTTACTGTGAGTAG) primers, respectively. Primers were engineered with terminal 5' CTCTCT sequences to facilitate subsequent restriction enzyme digestion and subcloning. The PCR product was cloned into the pSRaSD7-GFP vector (provided by Dan Denney; Figure 4.3) immediately 5' to the splice donor/acceptor regions to produce p5'IL2-GFP (Figure 4.4). The GFP used in this vector encoded for a mutant of the wildtype GFP gene which encodes a serine to threonine mutation at amino acid 65 that causes GFP to exhibit a single emission peak between 470-490nm that is four- to six-fold greater than the wildtype protein (164).

A 114 base sequence of single stranded DNA corresponding to a trimerized repeat of the human NFAT binding domain of the IL2 gene was synthesized on 1000 Angstrom deoxy-adenine CPG (Glenn Research, Sterling, VA, U.S.A) using an Applied Biosystems Model 391 DNA Synthesizer (Table 2.1). Crude oligonucleotide was cleaved off the resin and reconstituted in TE and half of this mixture was mixed with an equal volume of 99% formamide. Full length ssDNA was purified from truncated oligonucleotides by denaturing polyacrylamide gel electrophoresis(10% gel: mM Tris, mM borate, mM EDTA, M urea). Purified ssDNA was converted to dsDNA by PCR with *Pfu* polymerase using the 5'NFAT 114 (CTCTCTAAGCTTGGAGGAAAA) and 3'NFAT 114 (CTCTCTCTG

CAGACGCCT) primers, which incorporated terminal Hind III and Pst I sites, respectively. The NFAT trimer was cloned into the Hind III and Pst I sites of the pBlueScript KS- vector (Stratagene) using techniques described in Materials and Methods.

A second PCR was amplified from p5'IL2-GFP beginning at base -70 relative to the IL-2 gene's transcriptional start site and extending to the 3' end of the GFP gene. Primers incorporated a 5' Pst I site (5' primer: CTCTCTCTGCAGCATTTTGACACCCCC CATAATAT) and a 3' Not I site (3' primer: GCGGCCGCTATTATTTGTATAGTTCATC CATGC). This subfragment was cloned 3' to the NFAT trimer in pBluescript KS-. The entire NFAT trimer, minimal IL-2 promoter, intervening splice donor and acceptor, and GFP gene were excised from pBluescript KS- by digestion with Hind III and Not I and shuttled to pSRαSD7 to produce $pNFAT_3$-GFP (Figure 4.5)

These constructs were to be stably transfected into the TCR negative variant of the BW 5147 T cell leukemia line. This line was chosen over the conventional TCR-bearing BW5147 line to reduce the chance that hybrids would express non-antigen specific TCR from the fusion partner itself. Initial attempts to transfect the $pNFAT_3$-GFP and p5'IL2-GFP constructs into the BW α–β– cell line by electroporation were unsuccessful due to use of the voltage settings for the parental BW 5147 (α+β+) cell line. A voltage curve was performed by electroporation of BW 5147 α–β– with a neomycin-encoding plasmid, pSSD5.neo, followed by incubation in geneticin. The optimum voltage of 200volts was determined based on a balance between the viability of the cells 24hrs post-transfection and the number of clones obtained (Figure 4.6).

Linearized $pNFAT_3$-GFP and p5'IL2-GFP were stably-transfected into BW 5147 α–β– and resulting clones were incubated with 10ng/ml PMA and 1μM ionomycin to assay for GFP inducibility. Combinations of PMA and ionomycin have previously been shown

to induce in lymphoid cell populations the expression of receptors for IL-2, the secretion of IL-2, and cell proliferation (165). Further, Fiering *et al* also made use of PMA/ionomycin in testing reporter gene inducibility in cells transfected with a trimer of NFAT directing lacZ expression (156). Initial stimulations identified two lines, NFAT-5 and 5'IL2-6, that fluoresced well compared to controls (Figure 4.7). At first, it seemed that GFPs inducible fluorescence levels were not sufficient to be used as a reporter. This underscores one of the potential drawbacks of GFP in comparison to the lacZ employed by Sanderson *et al* : GFP is not enzymatic in nature and therefore does not afford the accumulation of a fluorescent product that increases the fluorescent signal. However, these two fusion partners had levels of fluorescence similar to that expressed in BW $\alpha-\beta-$ transfected with pSRaSD7-GFP (which utilizes a constitutive promoter to direct GFP expression; Figure 4.7b), although the number of cells expressing this level of fluorescence was lower for the cells employing the NFAT-5.5 and 5'IL2-6.6 constructs. To address this issue, these fusion partners were restimulated with PMA/ionomycin and cells from the brightest 5% were single cell cloned by FACS in order to create a population with a stronger level of inducible fluorescence. A second reason for cloning these lines was to try and select for a stable cell population as repeated screening of transfectants over the course of time had shown that the fluorescence level of some lines would drop in intensity, despite the fact that under the conditions used, electroporation should produce stably-transfected cells. Cloned cells were again restimulated with PMA/ionomycin to identify the brightest clones, NFAT-5.5 and 5'IL2-6.6. Figures 4.7d and 4.7f show that single-cell cloning did not achieve the desired effects of increasing both the number of stimulated cells and their level of fluorescence. Furthermore, the NFAT-based construct exhibited a better fluorescence profile as compared to its 5'IL2 promoter counterpart prior to sorting; however, both constructs yielded comparable levels of GFP inducibility after single cell cloning. The

cloned fusion partners were chosen for further analysis in T cell hybridoma production.

T cell hybridomas were initially produced by fusion of these cells with T cells from NOD mice immunized with hGAD65. These hybridomas were used to test GFP inducibility by antigen-independent anti-CD3 and PMA/ionomycin stimulation. These T cell stimulation techniques were chosen because they omitted APCs from subsequent FACS analysis, minimizing any potential non-specific fluorescence they may impart, and to ensure maximal T cell stimulation. Initial results did not reveal detectable GFP. However, a plot of the side scatter height (SSC-H) of light versus the forward scatter height of light (FSC-H) as cells pass through the FACS machine suggested that there was extensive cell death in the stimulated cells in comparison to controls (Figure 4.8). FSC and SSC are related to the size and membrane surface qualities of cells. Dead cells are typically associated with region I and live cells with region II, as marked on Figure 4.8a. Previous reports have shown that activation of T cell hybridomas, whether by antigen or polyclonal stimulators, induces Fas/Fas ligand mediated death (for review see reference 166) of murine T cell hybridomas via apoptosis. This presented a significant problem to this construct's use not only as a T cell activation marker, but as a reporter that could be used to FACSort in vivo activated cells. If cells were apoptosing, it would be impossible to analyze whole cells for GFP content, let alone recover them. Additionally, GFP65T's fluorescence is not as bright as that as of FITC, necessitating FACS analysis as opposed to a plate reader, which would have been able to detect GFP in both cells and the cellular fragments resulting from apoptosis. Brunner *et al* have utilized human soluble Fas-immunoglobulin fusion protein (sFasIg), consisting of the human Fas receptor fused to the constant region of the (mouse/human) IgG molecule, to block Fas/Fas ligand interactions and inhibit activation-induced cell death (AICD) in activated murine T cell hybridomas (167). Based on this study, we decided to test the ability of human sFasIg produced in our laboratory to inhibit AICD in murine hybridomas stimulated by PMA/ionomycin. Although

there was a question of whether human sFasIg would work with murine cells, it is worthwhile to note that Brunner *et al* made use of human sFasIg for their studies on AICD in murine hybridomas. Hybrid lines were restimulated in the presence of sFasIg but, again, no significant amount of GFP could be detected. Unfortunately, though, the antigen-specificity of these hybridomas had not been tested, raising doubts as to whether the lack of GFP inducibility was due to an lack of T cell antigen recognition or to more downstream events associated with initiation of transcription or a problem with GFP itself.

We readdressed this question using modifications to the original procedure. It was observed that the NFAT-5.5 fusion partner gave high numbers of hybridomas after fusion as well as the fastest growing cultures; it was therefore used exclusively in the second set of experiments. In order to test antigen-mediated GFP inducibility in this fusion partner, NOD mice were immunized with OVA and draining lymph node cells were fused with NFAT 5.5. OVA was chosen as an immunogen during these experiments based on its potentially large number of T cell epitopes and the fact that there is a known, immunodominant OVA epitope in NOD mice. As the arbitrary loss of chromosomes is a consequence of the fusion process between multiple cells as the resulting hybrid stabilizes, fused cells were immediately plated out in selection medium containing 600μg/ml geneticin to encourage retention of the chromosome where the $pNFAT_3$-GFP construct had integrated. Antigen specific hybridomas were identified by antigen presentation assay with NOD splenocytes followed by ELISA to detect IL-2. The IL-2 produced by the two most responsive lines are shown in Table 4.1. The presence of the genomic DNA-integrated $NFAT_3$-GP construct within these lines was confirmed by PCR from these cells (Figure 4.9). The ability of sFasIg to inhibit AICD was tested by stimulating T cells with PMA/ionomycin in the presence and absence of 25μg/ml sFasIg were compared to unstimulated controls for evidence of apoptosis. Apoptosis was measured by propidium

iodide (PI) staining. PI is a dye which fluoresces upon intercalating into DNA. As such, it provides an indication of cellular DNA levels, ranging from diploidy to polyploidy, depending upon cell cycle status. During apoptosis, DNA is nicked and fragments extruded from the cell, resulting in cells that contain less than 2n amounts of DNA. Surprisingly, inclusion of sFasIg in T cell stimulation cultures was not found to significantly reduce the apoptotic cell population (Figure 4.10). More surprising is the observation that there was only a marginal increase in the percentage of apoptotic cell population upon PMA/ionomycin stimulation relative to non-stimulated controls. This appears to be in opposition to published reports on the effects of PMA and calcium ionophores on T cell hybridomas.

The results obtained in testing sFasIg's ability to block AICD were obtained retrospective to the stimulation of the OVA-specific T hybridomas with either anti-CD3 antibody or with PMA/ionomycin, in the presence of 25μg/ml sFasIg. FACS analysis 24 hours later showed that there was no significant increase in T cell fluorescence (Figure 4.11). In order to be sure that the PMA/ionomycin and anti-CD3 treatments were activating the T cells, culture supernatants from the T cell stimulations were assayed for IL-2. The IL-2 released exceeded the upper limit detection of the ELISA assay, suggesting that the T cells had been activated. An FSC versus SSC plot of the PMA-stimulated cells reveals no change in the "live" cell population upon exposure to PMA/ionomycin relative to controls. This finding is opposite to that found with hybridomas produced to hGAD65 previously (figure 4.8) and the reason for this is not readily apparent. Most importantly, the large number of live cells (Figure 4.12) enabled GFP, if it was present at any detectable level, to be measured (Figure 4.11).

Conclusion

The production of a GFP-inducible fusion partner, produced from the stable transfection of GFP linked to a minimal IL-2 promoter, did not work. The lack of GFP inducibility even upon antigen-independent stimulation is puzzling. It is not likely that the gated population of cells in Figure 4.12 would still contain apoptotic cells after a period of 24 hours, since the kinetics of apoptosis are much more rapid. One might argue that cells that had actually expressed GFP had died by AICD, and that the GFP was localized to small remnants of the cell which had escaped detection by FACS. This is unlikely as the proportion of live cells in the control and stimulated samples was essentially similar between the three populations tested and even gated analysis of all the events in the SSC vs FSC plot, including very small sized particles or fragments, revealed no increase in cellular fluorescence relative to controls (Figure 4.11).

One question that can be asked is if the T cells are actually being triggered and, if so, is the induced GFP being being degraded within the cell. The first part of this question has been addressed above by examining IL-2 levels of cultures of T cells stimulated with PMA/ionomycin and anti-CD3 crosslinking. With respect to GFP stability, previous mention of GFPs stability to a variety of conditions has been noted (161). Also, the fact that GFP can be detected in the straight transfected fusion partner cell lines up to 48hrs after stimulation suggests that the intracellular milieu of T cells is not inhospitable towards this protein. One might be tempted to argue that the chromosome that contains the integrated $NFAT_3$-GFP construct may have been dropped as the hybridomas stabilized. Since PCR could detect the GFP gene in the NO6 and NO8 hybridomas, this is unlikely.

Further, it is odd that combinations of PMA/ionomycin can be used to test GFP inducibility in the fusion partner alone, but upon fusion with an antigen primed lymphocyte, PMA/ionomycin is no longer able to stimulate these cells. The basis for this

loss of stimulatory capability is unclear. The fact that IL-2 is produced indicates that NFAT is being produced and is engaging its normal, endogenous DNA binding site.

One explanation that may be offered to account for this apparent contradiction in GFP expression in fusion partners and hybridomas may have to do with the nature of the fusion partner itself. BW α–β– was produced by mutagenesis to select for cells that lacked TCR expression (168). Mutagenesis may have resulted in defective expression of a gene product that is required for negative regulation of IL-2 gene transcription, allowing PMA/ionomycin stimulation to effect GFP production. Upon fusion with normal T cells from immunized mice, genetic complementation restores expression of this negative regulatory product. This gene product may be responsible for controlling transcriptionally-active levels of NFAT in T cells. Such a mechanism has been implicated as a factor in the dichotomy of IL-2 expression amongst Th1 and Th2 cells, whereby IL-2 producing Th1 cells have been shown to express transcriptionally active levels of NFAT that permit IL-2 production while Th2 cells do not (169). Expression of the protein synthesis initiation factor in murine Th2 cells was able to restore transcription directed from a $NFAT_3$-lacZ construct in these cells. The principle of genetic reconstitution by somatic cell hybridization has been previously used between BW α–β– and lymph node cells to restore coupling of the CD3 ζ chain to the mobilization of calcium in the former cell population (170).

Future Direction

If future work on the viability of GFP as a reporter of T cell activation is to be performed one could consider repeating these experiments carrying alongside the GFP construct another fusion partner stably transfected with a plasmid that encodes for cell surface expression of a non-T cell related protein that would be expressed on the surface of

T cells after stimulation. This may be a more practical idea in that detection of such a protein by FITC-labelled antibody imparts a higher level of fluorescence compared to that available with GFP65T. Alternatively, more recent, modified versions of GFP could be cloned into the current constructs. A combination of optimized codon usage and DNA shuffling has been used to construct a improved version of GFP with 45-fold increase in fluorescent relative to the wildtype GFP (171). Use of this GFP would not only facilitate detection by FACS, but by fluorescent plate readers as well. While questionable results were obtained with sFasIg produced in our laboratory, they did not impact on the analysis of GFP inducibility. Regardless, the functional qualities of the sFasIg may warrant investigation not only for its application in studies with these GFP constructs but also for its use in other models of T cell activation. Lastly, if this technology does not work, the ability to identify cross-reactive environmental antigens could be pursued by immunization of NOD mice with purified, recombinant proteins, such as the P2-C protein of coxsackie virus followed by production of T cell hybridomas. Antigen specific clones could then be tested for response to diabetes- or beta cell-associated autoantigens. One drawback of this approach is prerequisite knowledge of the specific cross reactive protein which, for a number of putative environmental triggers, remain largely uncharacterized.

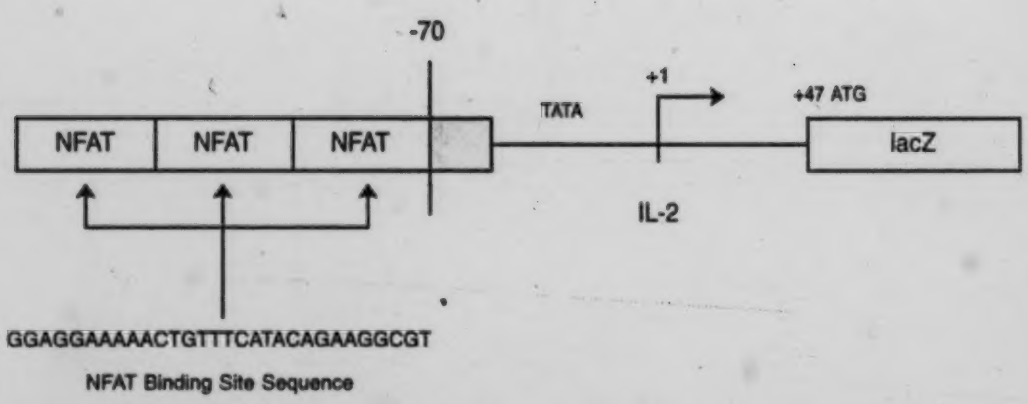

FIGURE 4.1. Schematic of $NFAT_3$-lac Z reporter construct. A tandem repeat of the human NFAT sequence is connected to a minimal human IL-2 promoter (-70 to +46) which directs transcription of the bacterial lacZ gene.

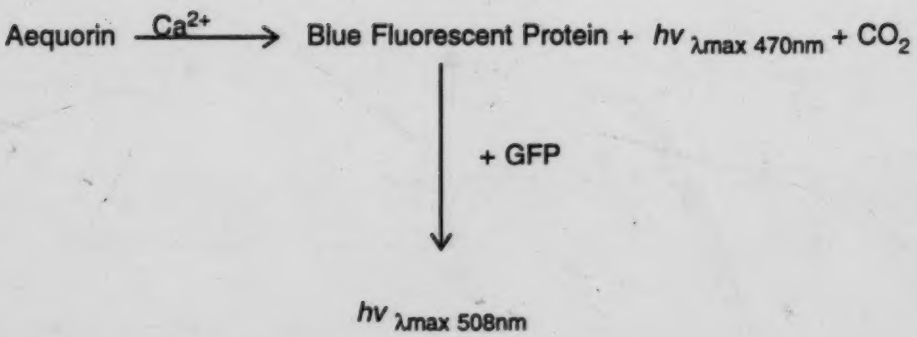

FIGURE 4.2. Schematic of fluorescence production in *Aequoria victoria.*

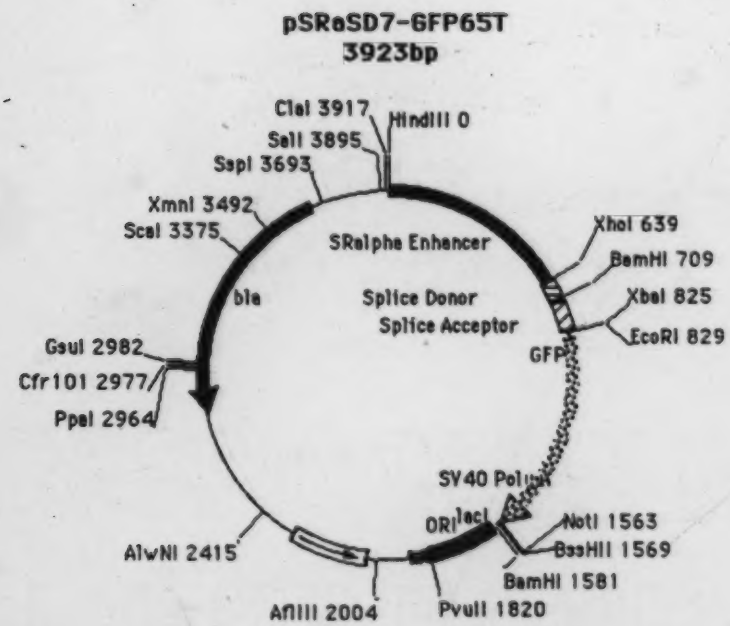

FIGURE 4.3 The pSRαSD7-GFP65T vector. pSRαSD7-GFP65T was provided by Dan Denney. The 717bp GFP65T insert is cloned into the Mlu I/Not I sites in the polylinker, and its expression is regulated by the constitutively-active SRα promoter.

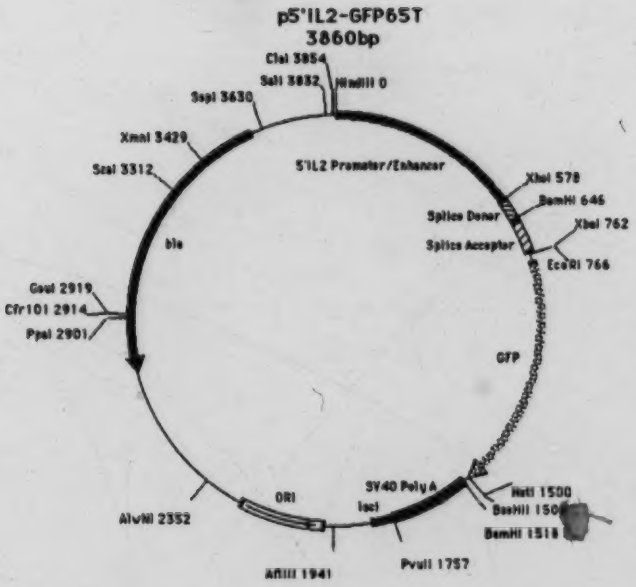

FIGURE 4.4 The p5'IL2-GFP65T vector. 5'IL2-GFP65T vector constructed by Hind III/Xho I digestion of pSRαSD7-GFP65T and Hind III/Xho I insertion of a 589bp 5' upstream region of the human IL-2 gene (bases -538 to +46), PCR amplified from genomic DNA using primers described in the text.

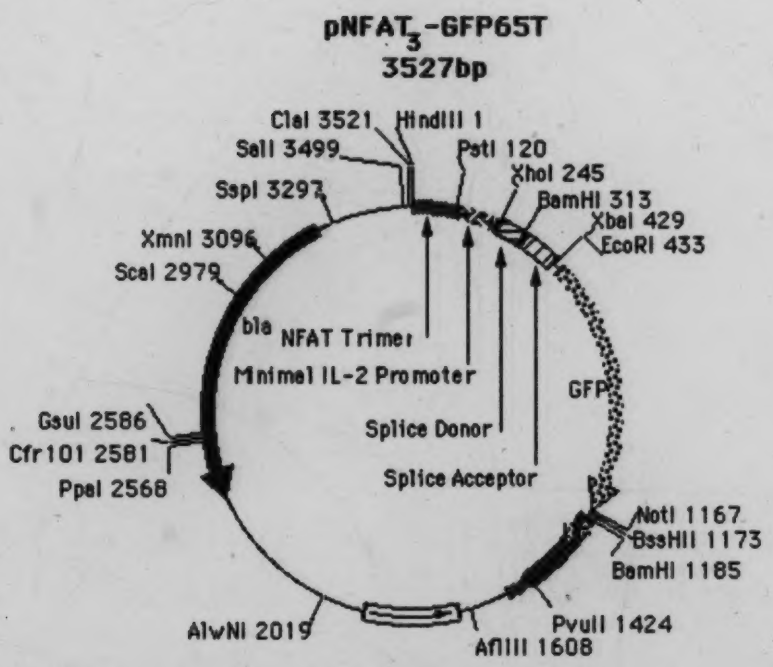

FIGURE 4.5 The pNFAT$_3$-GFP65T vector. The NFAT$_3$-GFP65T vector was constructed by first cloning a 114bp DNA fragment encoding a tandem NFAT trimer into the Hind III/Pst I sites of pBluescript KS-. A second piece of DNA was amplified by PCR from 5'IL2-GFP65T, corresponding to the -70 region of the IL-2 upstream region to the 3' end of the GFP gene. This PCR added a Pst I site to the 5' end and a Not I site to the 3' end; see text. This piece of DNA was cloned downstream of the NFAT trimer into the Pst I/Not I sites of pBluescript KS-. The entire NFAT$_3$-GFP65T region was excised from pBluescript KS- and shuttled to pSRαSD7-GFP65T linearized at Hind II/Not I sites, to create NFAT$_3$-GFP65T.

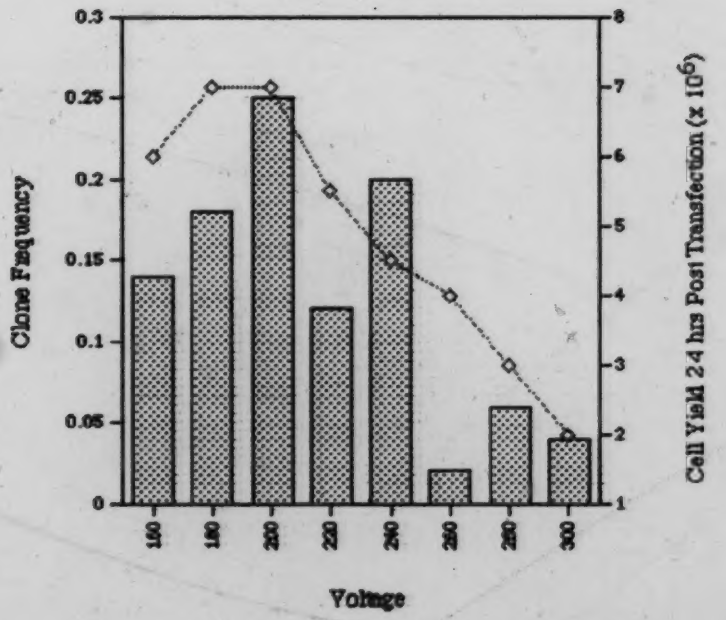

FIGURE 4.6. Change in BW α–β– cell viability and cloning efficiency with increasing electroporation voltages. BW α–β– cells ($1x10^7$) were transfected with 20μg of Sal I-linearized pSSD5.neo at various voltages. Cells were counted 24 hrs later, immediately preceding plating out and cell yields were expressed as a function of electroporation voltage.

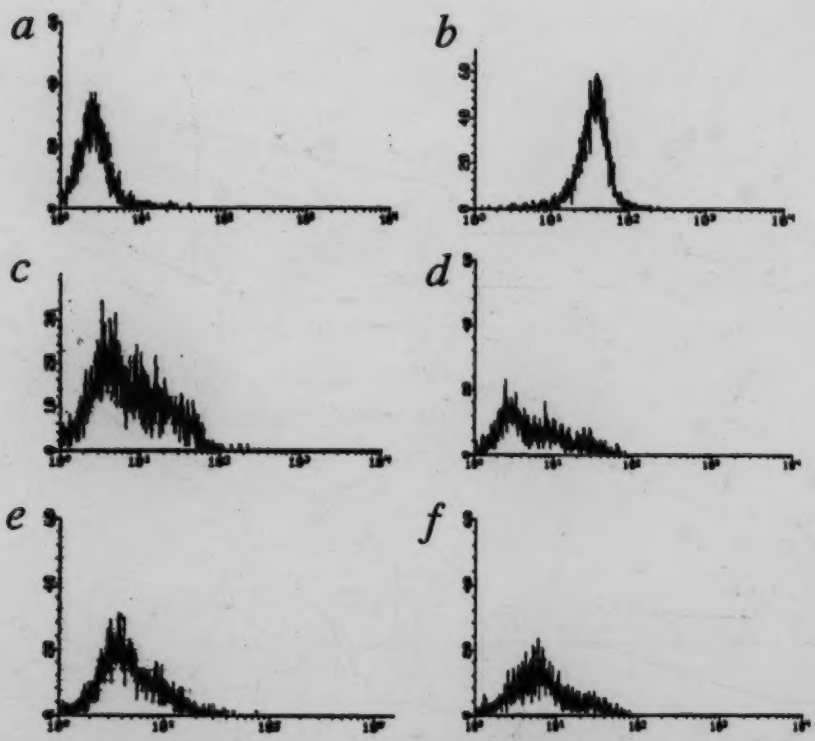

FIGURE 4.7. GFP induction in BW α–β– stably transfected with different GFP-containing vectors. BW α–β– cells were transfected with either pSRαSD7-GFP65T **(b)**, $NFAT_3$-GFP65T **(c and d)**, or 5'IL2-GFP65T **(e and f)** by electroporation and stimulated with PMA/ionomycin for 24hrs as described in the text. The GFP-related fluorescence of the brightest transfectant for each construct is shown: **a)** non-transfected BW α–β–, **b)** pSRαSD7-GFP65T transfectants (constitutive expression), **c)** NFAT-5 prior to single-cell cloning, **d)** the NFAT-5.5 clonal fusion partner, **e)** 5'IL2-6 prior to single-cell cloning, and **f)** the 5'IL2-6.6 clonal fusion partner. Fluorescene values for NFAT-5.5 and 5'IL2-6.6 were identical to that shown for BW α–β–.

TABLE 4.1. IL-2 Produced by NOD-Restricted, OVA-Specific T cell Hybridoma Lines.*

T cell line	Il-2 Produced (Units/ml)
NO-6	43.6
NO-8	9.1

*T cells ($1x10^5$)were incubated with NOD splenocyte APCs ($2x10^5$) and 40μg/ml OVA for 24 hrs in a volume of 200μl. Culture supernatants (75μl)were assayed for IL-2 by ELISA, as described in Materials and Methods. Negative controls consisting of T hybridoma cells incubated with APCs alone did not produce IL-2 beyond assay background levels.

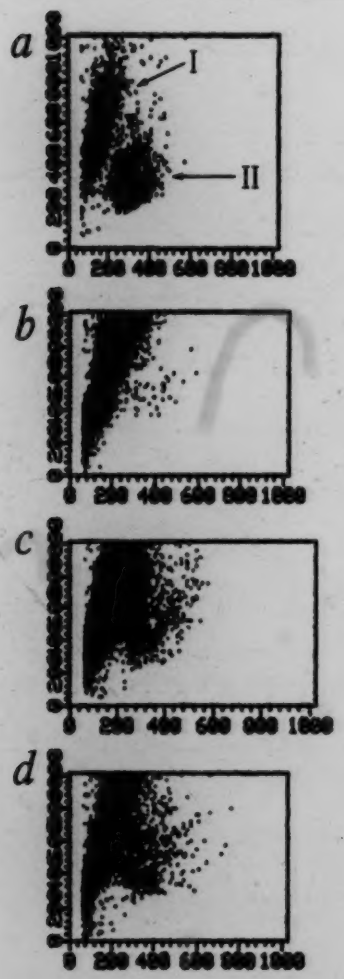

FIGURE 4.8. SSC-H vs FSC-H plot of T cells stimulated with PMA/ionomycin. $2x10^5$ T hybridoma cells produced by fusion of the NFAT-5.5 fusion partner with draining lymph node cells from NOD mice immunized with hGAD65 were **a)** untreated, or **b-d)** stimulated with immobilized anti-CD3. Cells were analyzed by FACS 24hrs later and SSC-H plotted versus FSC-H. Region I indicates the dead/dying cell population based on changes in membrane topology while region II points to the viable cell population. The results of three representative lines are shown **(b-d)**.

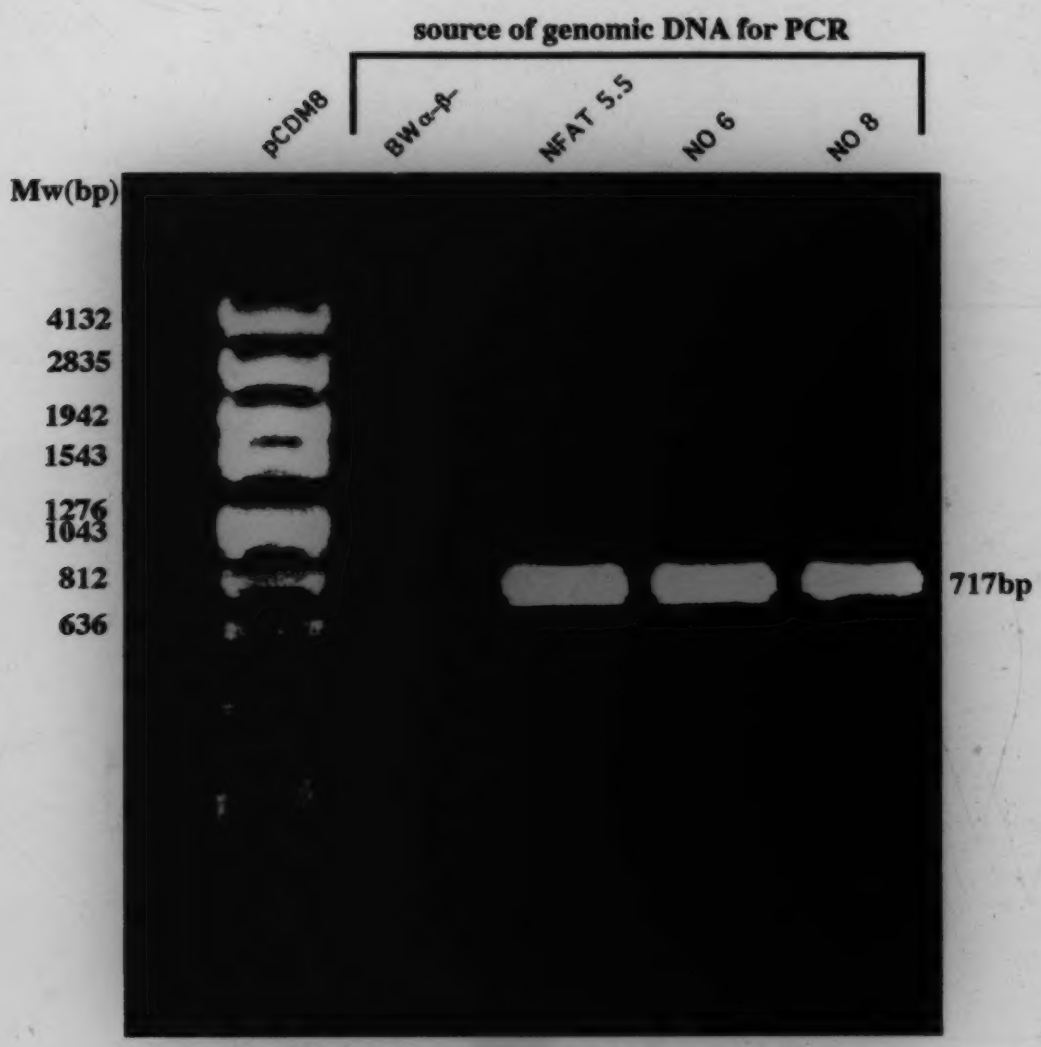

FIGURE 4.9. PCR-detection of GFP gene retention in NOD-restricted, OVA-specific T hybridoma lines 6 and 8. $1x10^4$ of the indicated cells were utilized for PCR amplification using the protocol and primers previously described in Materials and Methods. BW α–β–is the parental fusion partner that has not been transfected with the GFP gene; NFAT-5.5 is derived from transfectoin of BW α–β– with the $NFAT_3$-GFP65T construct; NO 6 and 8 are non-clonal T cell hybridomas produced by fusion of NFAT-5.5 with draining lymph node cells from OVA-immunized NOD mice. The base pair sizes of individual bands of the pCDM8 marker are shown above as is the size of the amplified GFP fragment. Primers used in this PCR are shown in Table 2.1.

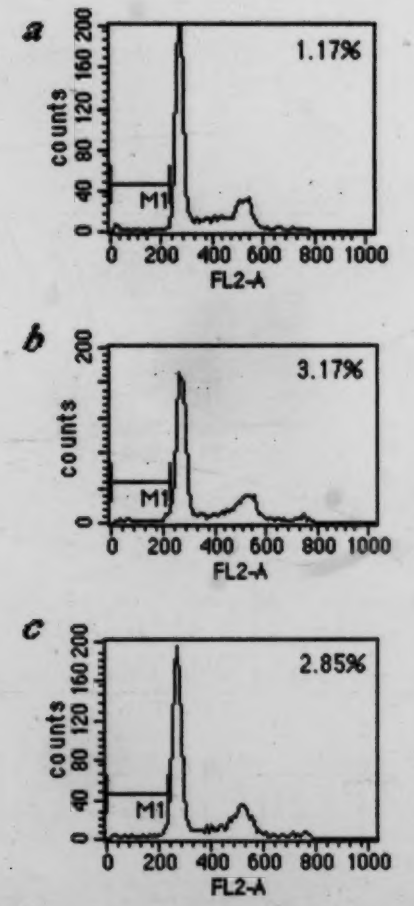

FIGURE 4.10. sFasIg does not appreciably decrease AICD in PMA/ionomycin stimulated T cells. $5x10^5$ NO 6 T hybridomas were either **a)** untreated, **b)** stimulated with PMA/ionomycin alone, or **c)** stimulated with PMA/ionomycin + 25μg/ml sFasIg. Cells were stained with propidium iodide 24 hrs later as described in Materials and Methods and the ratio of subdiploid cells expressed as a percentage of the total number of cells anayzed.

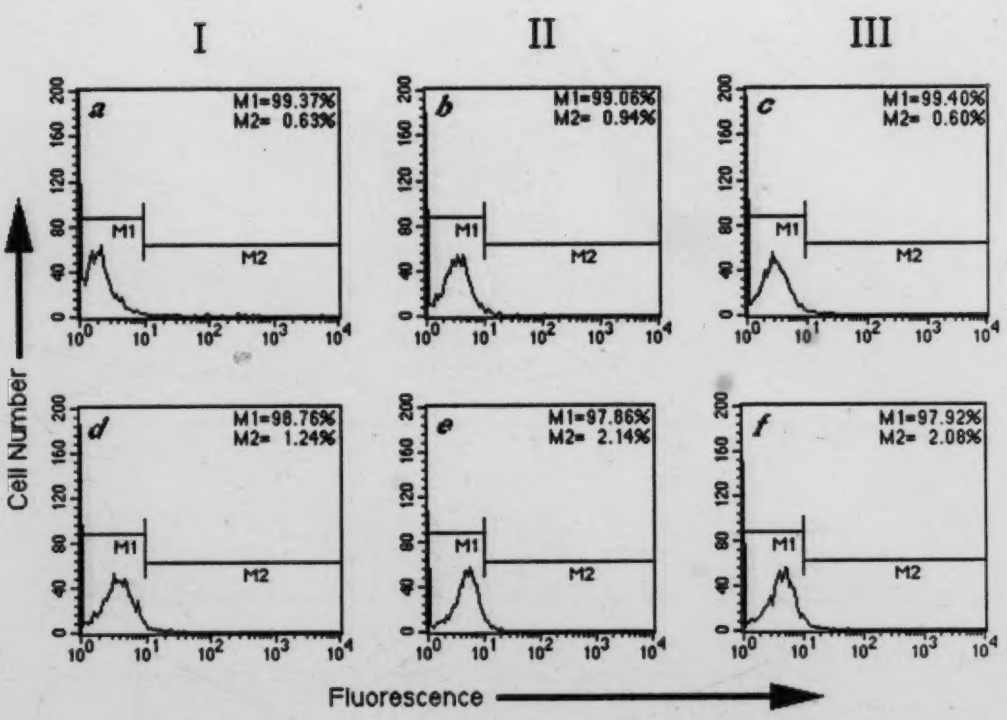

FIGURE 4.11. GFP is not detectable in OVA-specific T hybridomas produced by fusion with NFAT 5.5. $2x10^5$ NO 6 **(columns I and II)** and NO 8 **(column III)** T cell hybridomas were either untreated **(a and d)**, or stimulated with immobilized anti-CD3 + 25μg/ml sFasIg **(b and c)** or with PMA/ionomycin + 25μg/ml sFasIg **(e and f)**. Cells were analyzed for GFP expression by FACS 24hrs later.

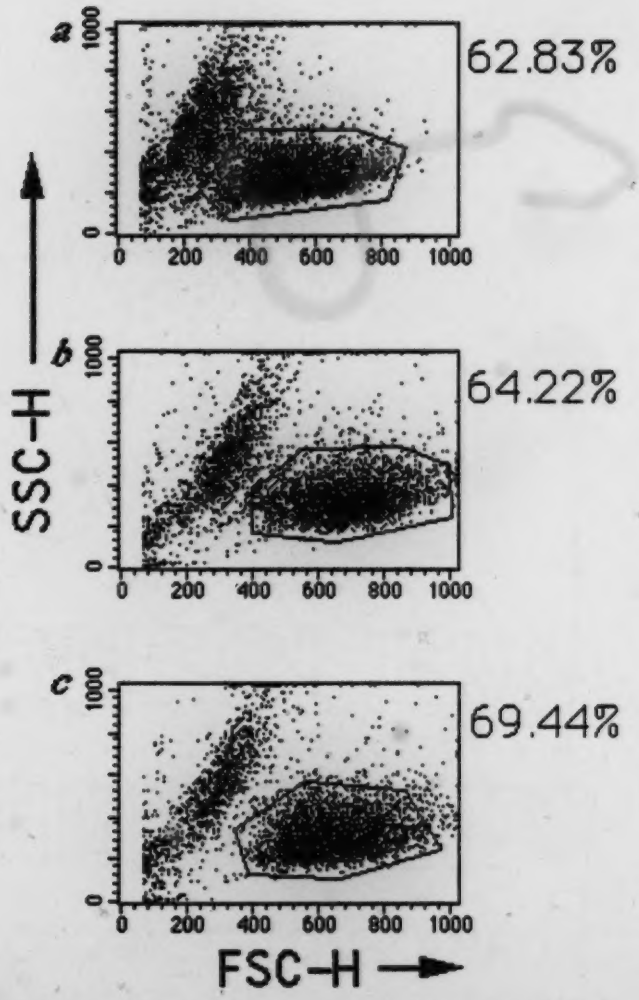

FIGURE 4.12. SSC-H vs FSC-H plot of OVA-specific T cell hybridomas stimulated with PMA/ionomycin. $2x10^5$ **a)** untreated NO 6 cells, **b)** NO 6 cells stimulated with PMA/ionomycin + 25µg/ml sFasIg, or **c)** NO 8 cells stimulated with PMA/ionomycin + 25µg/ml sFasIg, were incubated for 24hrs. SSC-H was plotted versus FSC-H and the percentage of live cells, demarcated by the G1 gate, was determined.

Chapter V

GENERAL DISCUSSION AND CONCLUSIONS

The goal of producing hGAD65-specific T cell hybridomas in NOD mice has been fulfilled. The peptide reactivity of one clone to an overlapping set of peptides to hGAD65 was shown to reside in aa of the protein. This peptide was found to share the previously defined class II I-A_{β}^{g7}-associated peptide binding motif. It will be interesting to compare these hGAD65 epitopes with those for HLA-DQ8, which are currently being delineated in our laboratory using transgenic mice. The implications of a possible association between epitopes would not only strengthen the principle behind using NOD mice for studyiing IDDM pathogenesis, but clarify avenues for using these hybridomas to devise strategies to modulate disease.

Development of a novel T cell fusion partner that incorporated a minimal IL-2 promoter to control expression of the GFP was not succesful. GFP was found to be inducible in the fusion partner, but not in T cell hybrids. If GFP is to explored as a reporter of T cell activation, future studies should employ not only improved versions of GFP, but also a positive control such as the construct used by Sanderson *et al* (154), or a non-T cell associated memebrane protein that would be expressed on the cell surface upon T cell activation.

The study of autoantigen T cell epitopes is necessary to uncover the underlying mechanisms that elicit IDDM such that future therapeutic modalities may be developed. Treatment may involve administering to susceptible or afflicted individuals variants of previously identified antigenic peptides whose amino acid sequence differs from the nominal peptide in one or two critical sites. These altered peptide ligands (APLs) contain

amino acid substitutions in the portion of the peptide that contacts the CDR3 region of the TCR. Since there are no changes in regions of the peptide that contact the MHC, binding to the MHC is preserved. APLs may only partially activate diabetogenic T cells (partial agonists) or may completely block the activating signal (antagonist peptide). Examination of cells exposed to partial agonists or antagonists reveals a characteristic pattern of CD3ζ chain phosphorylation which differs from that observed in fully activated cells (56, 172). Consequently, ZAP-70 fails to be recruited and T cell activation is compromised. Conceptually, APLs would be administered to individuals whose T cells respond to particular diabetes autoantigens in order to inactivate them.

The application of APLs to the treatment of autoimmune diseases has been investigated by several groups. In one study focusing on MS, incubation of isolated human T cell clones reactive to a key MS autoantigen, myelin basic protein, was shown to change the T cell cytokine secretion profile from that promoted disease to one that did not (173).

Another possible treatment for autoimmune disease extends the application of APLs to autoimmune therapy even further, relying on the delivery of soluble class II molecules loaded with APLs to patients. Production of soluble class II molecules has been typically limited to bulk purification of class II molecules from the APCs since the hydrophobic transmembrane region would direct recombinantly-synthesized class II to the plasma membrane. More recently, however, replacement of the transmembrane regions with leucine zipper motifs has enabled recombinant class II molecules to not only pass through the plasma membrane, but to also assume a correctly folded and assembled structure (174). Kozono *et al* have extended this principle even further by engineering the expression of a soluble I-$E^{d/k}$- and I-A^{d}-peptide complex by incorporating the DNA sequence of the peptide into the open reading frame of the class II molecule (175). The 'binding' peptide is separated from the amino-terminal end of the β-chain by a flexible linker segment. Fremont

et al subsequently used this technique to determine the x-ray crystal structure for the murine I-E(k) class II molecule occupied with a peptide (176). The use of APLs linked to diabetes-associated class II molecules is particulary attractive for two reasons. First, by attaching the antagonistic peptide to the appropriate class II, concern over the amount of peptide that actually associates with class II on APCs is obviated. Secondly, the use of soluble class II-peptide complexes to stimulate T cells in the absence of a costimulatory signal induce T cell anergy in potentially autoreactive T cells.

These strategies, while encouraging from in vitro and animal studies, are not without limitations and their capacity to modulate autoimmune disease in humans remains to be proven. Autoimmune diseases such as IDDM and MS are caused by disease inducing T cells sequestered in their target organs (pancreatic β-cells or brain, respectively), which mediate damage both specifically by direct cytotoxic T cell function and non-specifically through the release of cytokines which themselves compromise tissues and recruit other inflammatory cells. Whether injected APLs or soluble class II-APL complexes will encounter these T cells within their target tissues is open to speculation. Furthermore, it has been noted that some peptides transiently associate with their cognate MHC molecules in rodent models of several diseases. Pearson *et al* have suggested that the affinity of a peptide for its specific class II molecule and the ratio of loaded versus non-loaded class II molecules formed during peptide therapy will influence the degree of disease amelioration (177). Consequently, the "on-off" kinetics of APL and MHC interactions in vivo must be considered if T cells are to have sufficient time to interact with peptide-MHC complexes. The use of linkers that covalently couple peptide to the class II molecule may address this concern to some degree. Finally, epitope spreading within an autoantigen may necessitate the use of multiple, defined APLs. Regardless of the approach used and the associated concerns, their success relies upon the definition of T cell epitopes in putative autoantigens and the manner in which they elicit disease.

BIBLIOGRAPHY

1. Dausset J. 1959. Iso-leuco-anticorps. *Acta Haematol* 20: 156

2. Bodmer JG, Marsh SGE, Albert ED, *et al.* 1994. Nomenclature for factors of the HLA system. *Hum Immunol* 41: 1-20

3. Parham P, Loman CE, Lawlor DA, *et al.* 1988. Nature of polymorphisms in HLA-A, -B, -C molecules. *Proc Natl Acad Sci USA* 85:4005-4009

4. Campbell RD, Trowsdale J. 1993. Map of the human MHC. *Immunol Today* 14:349-352

5. Bjorkman, PJ, Parham P. 1990. Structure, function, and diversity of class I major histocompatibility molecules. *Annu. Rev. Biochem.* 59: 253-288

6. Goodfellow PN, Jones EA, van Heyningen V, *et al.* 1975. The beta-2-microblobulin gene is on chromosome 15 nad not in the HL-A region. *Nature* 254:261-269

7. Wei X, Orr HT. 1990. Differential expression of HLA-E, HLA-F, and HLA-G transcripts in human tissue. *Hum Immunol* 29: 131

8. Shimizu Y, Geraphty DE, Koller BH, *et al.* 1988. Transfer and expression of three cloned human non HLA-A, B, C class I major histocompatibility complex genes in lymphoblastoid cells. *Proc Natl Acad Sci USA* 85:227-231

9. Kaufman JF, Auffray C, Korman AJ, *et al.* 1984. The class II molecules of the human and murine major histocompatibility complex. *Cell* 36: 1-13

10. Gustafsson K, Widmark R, Jonsson K, *et al.* 1987. Class II genes of the major histocompatibility complex. Evolution of the DP region as deduced from nucleotide sequences of the four genes. *J Biol Chem* 262:8778-8786

11. DeMars R, Spies T. 1992. New genes in the MHC endcode proteins for antigen processing. *Trends Cell Biol* 2: 81

12. Carroll MC, Katzman P, Alicot EM, *et al.* 1987. Linkage map of the human major histocompatibility complex including the tumour necrosis factor genes. *Proc Natl Acad Sci USA* 84:8535-8539

13. Hansen TH, Carreno BM, Sachs DH. 1993. *In* "Fundamental Immunology" (WE Paul ed.), pp. 577-628. Raven Press, Ltd., New York

14. Daar AS, Fuggle SV, Fabre JW, *et al.* 1984. The detailed distribution of the HLA-A, B, C antigens in normal human organs. *Trasnplantation* 38: 287-292

15. Daar AS, Fuggle SV, Fabre JW, *et al.* 1984. The detailed distribution of MHC class II antigens in normal human organs. *Trasnplantation* 38: 293-298

16. Tucker C, Korman AJ, Wake CT, *et al.* 1984. Immune interferon activates multiple class II major histocompatibility complex genes and the associated invariant chain gene

in human endothelial cells and dermal fibroblasts. *Proc Natl Acad Sci USA* 81:4917-4921

17. Chang, C-H, Fontes DJ, Peterlin M, *et al.* 1994. Class II transactivator (CIITA) is sufficient for the inducible expression of major histocompatibility complex class II genes. *J. Exp. Med.* 180:1367-1374

18. Germain RN. 1993. The biochemistry and cell biology of antigen processing and presentation. *Annu. Rev. Biochem.* 11: 403-450

19. Bjorkman, PJ, Parham P. 1990. Structure, function, and diversity of class I major histocompatibility molecules. *Annu. Rev. Biochem.* 59: 253-288

20. Bjorkamn PJ, Saper MA, Samraoui B, *et al.* 1987. Structure of the human class I major histocompatibility antigen HLA-A2. *Nature* 329:506-512

21. Garrett TP, Saper MA, Bjorkman PJ, *et al.* 1989. Specificity pockets for the side chains of peptide antigens in HLA-Aw68. *Nature* 342: 692-696

22. Fremont DH, Matsumura M, Stura EA, *et al.* 1992. Crystal structures of two viral peptides in complex with murine MHC class I H-2K^b. *Science* 257: 919-927

23. Kappes D, Strominger JL. 1988. Human class II major histocompatibility complex genes and proteins. *Annu. Rev. Biochem.* 57: 991-1028

24. Brown JH, Jardetsky TS, Gorga JC, *et al.* 1993. Three-dimensional structure of the human class II histocompatibility antigen HLA-DR1. *Nature* 364: 33-39

25. Rudensky AY, Preston-Hurlburt P, Hong SC, *et al.* 1991. Sequence analysis of peptides bound to MHC class II molecules. *Nature* 353: 622-627

26. Hunt DF, Michel H, Dickinson TA, *et al.* 1992. Peptides presented to the immune system by the murine class II major histocompatibility complex molecule I-A^d. *Science* 256: 1817-1820

27. Chicz RM, Urban RG, Gorga JC, *et al.* 1992. The predominant naturally processed peptides bound to HLA-DR1 are derived from MHC-related molecules and are heterogenous in size. *Nature* 358: 764-768

28. Gething MJ, Sambrook J. 1992. Protein folding in the cell. *Nature* 355: 33-45

29. Vassilakos A., Cohen-Doyle MF., Peterson PA., Jackson MR., Williams DB. 1996. The molecular chaperone calnexin facilitates folding and assembly of class I histocompatibility molecules. *EMBO Journal* 15: 1495-506

30. Sadasivan B., Lehner PJ., Ortmann B., Spies T., Cresswell P. 1996. Roles for calreticulin and a novel glycoprotein, tapasin, in the interaction of MHC class I molecules with TAP. *Immunity.* 5: 103-14

31. Lehner PJ., Cresswell P. 1996. Processing and delivery of peptides presented by MHC class I molecules. *Current Opinion in Immunology.* 8: 59-67

32. Neefjes JJ, Stollorz V, Peters PJ, *et al.* 1990. The biosynthetic pathway of MHC class II but not class I molecules intersects the endocytic route. *Cell* 61: 171-183

33. Jones PP, Murphy DB, Hewgill D, *et al.* 1979. Detection of a common polypeptide chain in I-A and I-E sub-region immunoprecipitates. *Mol. Immunol.* 16: 51-60

34. Strubin M, Berte C, Mach B. 1986. Alternative splicing and alternative initiation of translation explains the four forms of the Ia antigen associated invariant chain. *EMBO J* 5:3483-3488

35. Roche PA., Teletski CL., Karp DR., Pinet V., Bakke O., Long EO. 1992. Stable surface expression of invariant chain prevents peptide presentation by HLA-DR. *EMBO Journal* 11: 2841-7

36. Bikoff EK., Huang LY., Episkopou V., van Meerwijk J., Germain RN., Robertson EJ. 1993. Defective major histocompatibility complex class II assembly, transport, peptide acquisition, and CD4+ T cell selection in mice lacking invariant chain expression. *JEM* 177: 1699-712

37. Pieters J., Bakke O., Dobberstein B. 1993. The MHC class II-associated invariant chain contains two endosomal targeting signals within its cytoplasmic tail. *J. Cell Biol.* 106: 831-46

38. Wolf PR., Ploegh HL. 1995. How MHC class II molecules acquire peptide cargo: biosynthesis and trafficking through the endocytic pathway. *Jannu Rev Cell Dev Biol.* 11: 267-306

39. Freisewinkel IM., Schenck K., Koch N. 1993. The segment of invariant chain that is critical for association with major histocompatibility complex class II molecules contains the sequence of a peptide eluted from class II polypeptides. *Proc Natl Acad Sci USA* 90: 9703-6

40. Sloan VS., Cameron P., Porter G., Gammon M., Amaya M., Mellins E., Zaller DM. 1995. Mediation by HLA-DM of dissociation of peptides from HLA-DR. *Nature*. 375: 802-6

41. Denzin LK., Cresswell P.1995. HLA-DM induces CLIP dissociation from MHC class II alpha beta dimers and facilitates peptide loading. *Cell*. 82: 155-65

42. Urban RG, Chicz RM, Vignali DA, *et al.* 1993. The dichotomoy of peptide presentation by class I and class II MHC proteins. *Chem. Immunol* 57:197-234

43. Falk K, Rötzschke O, Rammensee HG. 1990. Cellular peptide composition governed by major histocompatibility complex class I molecules. *Nature* 348:248-251

44. Rötzschke O, Falk K, Deres K, *et al.* 1990. Isolation and analysis of naturally processed viral peptides as recognized by cytotoxic T cells. *Nature* 348:252-254

45. VanBleek GM, Nathenson SG. 1990. Isolation of an endogenously processed immunodominant viral peptide from the class I H-2K^b molecule. *Nature* 348:213-216

46. Rudensky A, Preston HP, Hong SC, *et al.* 1991. Sequence analysis of peptides bound to MHC class II molecules. *Nature* 353:622-627

47. Hunt DF, Michel H, Dickinson TA, *et al.* 1992. Peptides presented to the immune system by murine major histocompatibility complex molecule I-A^d. *Science* 256:1817-1820

48. Harding CV, Unanue ER. 1990. Cellular mechanism of antigen processing and the function of class I and II major histocompatibility complex molecules. *Cell Reg* 1:499-509

49. Nuchtern JG, Bonifacino JS, Biddison WE, *et al.* 1989. Brefeldin A implicates egress from endoplasmic reticulum in class I restricted antigen presentation. *Nature* 339:223-226

50. Nuchtern JG, Biddison WE, Klausner WD. 1990. Class II MHC molecules can use the endogenous pathway of antigen presentation. *Nature* 343:74-76

51. Jin Y, Shi J, Berkowar I. 1988. Human T cell response to the surface antigen of Hepatitis B virus (HBsAg). *J. Exp. Med.* 168:293-306

52. Pfeifer JD, Wick MJ, Roberts RL, *et al.* 1993. Phagocytic processing of bacterial antigens for class I MHC presentation to T cells. *Nature* 361:359-362

53. Clevers H, Alarcon B, Wileman T, *et al.* 1988. The T cell receptor/CD3 complex: a dynamic protein ensemble. *Annu Rev Immunol* 6:629-662

54. Haas W, Kaufman S, Martinez AC. 1990. The development and function of T cells. *Immunol Today* 11:340-343

55. Novotny J., Tonegawa S., Saito H., Kranz DM., Eisen HN. 1986. Secondary, tertiary, and quaternary structure of T-cell-specific immunoglobulin-like polypeptide chains. *Proc Natl Acad Sci USA*. 83: 742-6

56. Kuby, J. *Immunology*, New York: W.H. Freeman & Company, 1997. Ed. 3

57. Davis, M.M., Bjorkman, P. 1988. T-cell antigen receptor gene and T-cell recognition. *Nature* 334: 395

58. Claverie., J.M.,Procknicha-Chalufour, A., Bougegueleret, L. 1989. Immunological implications of a Fab-like structure of the T-cell receptor. *Immunol Today*. 10: 10

59. Garcia KC., Degano M., Stanfield RL., Brunmark A., Jackson MR., Peterson PA., Teyton L., Wilson IA. 1996. An αβ T cell receptor structure at 2.5 A and its orientation in the TCR-MHC complex. *Science* 274: 209-19

60. Benoist, C., Mathis, D. 1989. Positive selection of the T cell repertoire: Where and when does it occur? *Cell* 58: 1027-1033

61. Von Boehmer, H. 1994. Positive selection of lymphocytes. *Cell* 76: 219-228

62. Nossal, G. 1994. Negative selection of lymphocytes. *Cell* 76: 229-239

63. Janeway, C.A. 1989. Immunogenicity signals 1,2,3 ... and 0. *Immunol Today* 10: 283

64. Liu., Y., Linsley, P.S. 1992. Co-stimulation of T-cell growth. *Curr. Opin. Immunol.* 4: 265

65. Wingren AG., Parra E., Varga M., Kalland T., Sjogren HO., Hedlund G., Dohlsten M. T cell activation pathways: B7, LFA-3, and ICAM-1 shape unique T cell profiles. *Crit Rev Immunol* 15: 235-253

66. Cammarota G, Schierle A, Takacs B, *et al.* 1992. Identification of a CD4 binding site on the 2 domain of of HLA-DR molecules. *Nature* 356:799-801

67. Janeway CA. 1991. The co-receptor function of CD4. *Semin Immunol* 3:153-160

68. Salter RD, Norment AM, Chen BJ, *et al.* 1989. Polymorphism in the 2 domain of HLA-A molecules affects binding to CD8. *Nature* 338:345-347

69. Davis MM, Bkorkman PJ. 1988. T-cell antigen receptor genes and T-cell recognition. *Nature* 334:395-402

70. Matis LA. 1990. The molecular basis of T-cell specificity. *Annu Rev Immunol* 8:65-82

71. Weiss, A., Littman, DR. 1994. Signal transduction by lymphocyte antigen receptors. *Cell* 76: 263-74

72. Iwashima M., Irving BA., van Oers NS., Chan AC., Weiss A. 1994. Sequential interactions of the TCR with two distinct cytoplasmic tyrosine kinases. *Science* 263: 1136-39

73. McKeon F. 1991. When worlds collide: immunosuppressants meet protein phosphatases. *Cell* 66:823-826

74. Henderson DJ, Naya I, Burdick RV, *et al.* 1991. Comparison of the effects of FK506, cyclosporin A and rapamycin on IL-2 production. *Immunol.* 73:316-321

75. Morris RE. 1992. Immunopharmacology of new xenobiotic immunosuppressive molecules. *Semin Nephrol* 12:304-314

76. Springer, T.A. 1990. Adehesion receptors of the immune system. *Nature* 346: 425-34

77. Moingeon P., Chang HC., Sayre PH., Clayton LK., Alcover A., Gardner P., Reinherz EL. The structural biology of CD2. *Immunol Rev* 111: 111-44

78. Freeman GJ., Borriello F., Hodes RJ., Reiser H., Hathcock KS., Laszlo G., McKnight AJ., Kim J., Du L., Lombard DB., *et al.* 1993. Uncovering of functional alternative CTLA-4 counter-receptor in B7-deficient mice. *Science* 262: 907-9

79. Freeman GJ., Gribben JG., Boussiotis VA., Ng JW., Restivo VA Jr., Lombard LA., Gray GS., Nadler LM. 1993. Cloning of B7-2: a CTLA-4 counter-receptor that costimulates human T cell proliferation. *Science* 262: 909-11

80. Azuma M., Ito D., Yagita H., Okumura K., Phillips JH., Lanier LL., Somoza C. 1993. B70 antigen is a second ligand for CTLA-4 and CD28. *Nature* 366: 76-9

81. Durand DB., Shaw JP., Bush MR., Replogle RE., Belagaje R., Crabtree GR. 1988. Characterization of antigen receptor response elements within the interleukin-2 enhancer. *Mol Cell Biol* 8: 1715-24

82. Altmann DM., Hogg N., Trowsdale J., Wilkinson D. 1989. Cotransfection of ICAM-1 and HLA-DR reconstitutes human antigen-presenting cell function in mouse L cells. *Nature* 338: 512-4

83. van Kooyk Y., van de Wiel-van Kemenade P., Weder P., Kuijpers TW., Figdor CG. 1989. Enhancement of LFA-1-mediated cell adhesion by triggering through CD2 or CD3 on T lymphocytes. *Nature* 342: 811-3

84. Johnson AH, Hurley CK, Hartzman RJ, *et al.* 1991. HLA: the major histocompatibility complex of man. *In* "Clinical diagnosis and management by laboratory methods." (JB Henry ed.) p. 761. WB Saunders Co., Philadelphia

85. Cooke A. 1990. An overview on possible mechanisms of destruction of the insulin-producing beta cell. *Curr topics Microbiol Immunol* 164:125-142

86. Castano L, Eisenbarth GS. 1990. Type-I diabetes: chronic autoimmune disease of human, mouse and rat. *Annu Rev Immunol* 8:647-679

87. Nepom GT. 1990. A unified hypothesis for the complex genetics of HLA association with IDDM. *Diabetes* 39:1153-1157

88. Bosi E, Bonifacio E, Bottazzo GF, *et al.* 1993. Autoantigens in IDDM. *Diabetes Reviews* 1:204-214

89. Atkinson MA, Maclaren NK. 1993. Islet cell autoantigens in insulin-dependent diabetes. *J. Clin. Invest.* 92:1608-1616

90. Michelsen B, Lernmark A. 1987. Molecular cloning of a polymorphic DNA endonucleus fragment associates insulin dependent diabetes mellitus with HLA-DQ. *J. Clin. Invest.* 79:1144-1152

91. Wolf E, Spencer KM, Cudworth AG. 1983. The genetic susceptibility to Type-I (insulin-dependent) diabetes: analysis of the HLA-DR association. *Diabetologica* 24:224-230

92. Nepom BS, Schwartz D, Palmer JP, *et al.* 1987. Transcomplementation of HLA genes in IDDM. HLA-DQ - and -chains produce hybrid molecules in DR3/4 heterozygotes. *Diabetes* 36:114-117

93. Nepom BS, Palmer J, Kim SJ, *et al.* 1986. Specific genomic markers of the HLA-DQ

subregion discriminate between DR4+ insulin-dependent diabetes mellitus and DR4+ seropositive juvenile rheumatoid arthritis. *J. Exp. Med.* 164:345-350

94. Thorsby E, Rønningen KS. 1993. Particular HLA-DQ molecules play a dominant role in determining susceptibility or resistance to Type 1 (insulin-dependent) diabetes mellitus. *Diabetologica* 36:371-377

95. Todd JA, Bell JI, McDevitt HO. 1987. HLA-DQ gene contributes to susceptibility and resistance to insulin-dependent diabetes mellitus. *Nature* 329:599-604

96. Awata T, Iwamoto Y, Matsuda A, *et al.* 1989. High frequency of aspartic acid at position 67 of IDDM of HLA-DQ chain in Japanese IDDM and non-diabetic subjects. *Diabetes* 38:90A

97. Ikegami H, Noma Y, Yamamoto Y, *et al.* 1989. Analysis of HLA-DQ sequence in Japanese patients with insulin-dependent diabetes mellitus. *Diabetes* 38:19A

98. Sanjeevi CB, Lybrand Tp, DeWeese C, *et al.* 1995. Polymorphic amino acid variations in HLA-DQ associated with systematic physical property changes and occurrence of IDDM. *Diabetes* 44:125-131

99. Marrack P, Kappler J. 1988. The T-cell repertoire for antigen and MHC. *Immunol. today* 9:308-315

100. Ashton-Rickhardt PG, Tonegawa S. 1994. A differential avidity model for T cell selection. *Immunol. Today* 15:362-366

101. Nepom GT. 1993. Immunogenetics and IDDM. *Diabetes Rev.* 1:93-103

102. Theofilopoulos AN. 1995. The basis of autoimmunity: part I Mechanisms of aberrant self-recognition. *Immunol. Today* 16:90-98

103. Atkinson MA, Bowman MA, Campbell L, *et al.* 1994. Cellular immunity to a determinant common to glutamate decarboxylase and coxsackie virus in insulin-dependent diabetes. *J. Clin. Invest.* 94:2125-2129

104. Tian J, Lehmann PV, Kaufmann DL. 1994. T cell cross-reactivity between coxsackievirus and glutamate decarboxylase is associated with a murine diabetes susceptibility allele. *J. Exp. Med.* 180:1979-1984

105. Baekkeskov S, Nielsen JH, Marner BT, *et al.* 1982. Autoantibodies in newly diagnosed diabetic children immunoprecipitate human pancreatic islet cell proteins. *Nature* 298:167-169

106 Baekkeskov S, Jan-Aanstoot H, Christgau S, *et al.* 1990. Identification of the 64K autoantigen in insulin-dependent diabetes mellitus as the GABA-synthesizing enzyme glutamic acid decarboxylase. *Nature* 347:151-156

107. Bu DF, Erlander MG, Hitz BC, *et al.* 1993. Two human glutamate decarboxylases GAD 65 and GAD 67, are each encoded by a single gene. *Proc Natl Acad Sci USA* 89:2115-2119

108. Erdo SI, Wolff J. 1990. Gamma-Aminobutyric acid outside the mammalian brain. *J. Neurochem.* 54:363-372

109. Hagoplan WA, Michelsen B, Karlsen AE, *et al.* 1993. Autoantibodies in IDDM primarily recognize the 65,000-M_r rather than the 67,000-M_r isoform of glutamic acid decarboxylase. *Diabetes* 42:631-636

110. Richter W, Shi Y, Baekkeskov S. 1993. Autoreactive epitopes defined by diabetes-associated human monoclonal antibodies are localized in the middle and C-terminal domains of the smaller form of glutamate decarboxylase. *Proc Natl Acad Sci USA* 90:2832-2836

111. Chen SL, Whiteley PJ, Freed DC, *et al.* 1994. Response of NOD congenic mice to a glutamic acid decarboxylase-derived peptide. *J. Autoimmunity* 7:635-641

112. Kaufman DL, Clare-Salzler M, Tian J, *et al.* 1993. Spontaneous loss of T-cell tolerance to glutamic acid decarboxylase in murine insulin-dependent diabetes. *Nature* 366:69-72

113. Tisch R, Yang XD, Singer SM, *et al.* 1993. Immune response to glutamic acid decarboxylase correlates with insulitis in non-obses diabetic mice. *Nature* 366:72-75

114. Atkinson MA, Bowman MA, Campbell L, *et al.* 1994. Cellular immunity to a determinant common to glutamate decarboxylase and coxsackie virus in insulin-dependent diabetes. *J. Clin. Invest.* 94:2125-2129

115. Lohmann T, David R, Leslie G, *et al.* 1994. Immunodominant epitopes of glutamic acid decarboxylase 65 and 67 in insulin-dependent diabetes mellitus. *Lancet* 343:1607-1608

116. Yoon JW, Austin M, Onodera T, *et al.* 1979. Isolation of a virus from the pancreas of a child with diabetic ketoacidosis. *N. Engl. J. Med.* 300:1173-1179

117. Yoon J-W, London WT, Curfman BL, *et al.* 1986. Coxsackie virus B4 produces transient diabetes in nonhuman primates. *Diabetes* 35:712-716

118. Chatterjee NK, Nejman C, Gerling I. 1988. Purification and characterization of a strain of coxsackievirus B4 of human origin that induces diabetes in mice. *J. Med. Virol.* 26:57-69

119. King ML, Shaikh A, Birdwell D, *et al.* 1983. Coxsackie-B-virus-specific IgM responses in children with insulin-dependent (juvenile-onset; type-I) diabetes mellitus. *Lancet* 1:1397-1399

120. Banatvala JE, Schernthaner G, Schober E, *et al.* 1985. Coxsackie B, mumps, rubella, and cytomegalovirus specific IgM response in patients with juvenile-onset insulin-dependent diabetes mellitus in Britain, Austria and Australia. *Lancet* 1:1409-1412

121. Rudy G., Stone N., Harrison LC., Colman PG., McNair P., Brusic V., French

MB., Honeyman MC., Tait B., Lew AM. 1995. Similar peptides from two beta cell autoantigens, proinsulin and glutamic acid decarboxylase, stimulate T cells of individuals at risk for insulin-dependent diabetes. *Mol Medicine*.1: 625-33

122. Abstracts of the Keystone Symposium on Tolerance and Autoimmunity, Abstract No. 13-19, 1997.

123. Reske-Kunz AB, Landais D, Peccoud J, *et al.* 1989. Functional sites on the A alpha chain. Polymorphic residues involved in antigen presentation to insulin-specific, Ab alpha:Ak beta-restricted T cells. *J. Immunol.* 143:1472-1481

124. Williams DB, Ferguson J, Gariepy J, *et al.* 1993. Characterization of the insulin A-chain major immunogenic determinant presented by MHC class II I-A^d molecules. *J. Immunol.* 151:3627-3637

125. Naquet P, Ellis J, Singh B, *et al.* 1987. Processing and presentation of insulin. I. Analysis of immunogenic peptides and processing requirements for insulin A loop-specific T cells. *J. Immunol.* 139:3955-3963

126. Naquet P, Ellis J, Tibensky D, *et al.* 1988. T cell autoreactivity to insulin in diabetic and related non-diabetic individuals. *J. Immunol.* 140:2569-2576

127. Virtanen SM, Rasanen L, Aro A, *et al.* 1991. I. Infant feeding in Finnish children less than 7 yr of age with newly diagnosed IDDM. Childhood diabetes in Finalnd study group. *Diabetes Care* 14:415-417

128. Daneman D, Fishman L, Clarson C, *et al.* 1987. dietary triggers of insulin-dependent diabetes in the BB rat. *Diabetes Res* 5:93-97

129. Glerum M, Robinson BH, Martin JM. 1989. Could serum albumin be the initiating antigen ultimately responsible for the development of onset insulin-dependent diabetes mellitus? *Diabetes Res* 10:103-107

130. Karjalainen J, Martin JM, Knip M, *et al.* 1992. A bovine albumin peptide as a possible trigger of onset insulin-dependent diabetes mellitus. *N. Engl. J. Med.* 327:302-307

131. Martin Jm, Trink B, Daneman D, *et al.* 1991. Milk proteins in the etiology of onset insulin-dependent diabetes mellitus (IDDM). *Ann Med* 23:447-452

132. Robinson BH, Dosch H-M, Martin JM, *et al.* 1993. A model for the involvement of MHC class II proteins in the development of Type-I (insulin-dependent) diabetes mellitus in response toovine serum albumin peptides. *Diabetologica* 36:364-368

133. Miyazaki I, Gaedigk R, Hui MF, *et al.* 1994. Cloning of human and rat p69 cDNA, a candidate autoimmune target in type I diabetes. *Bioch. Biophys. Acta* 1227:101-104

134. Wicker LS., Todd JA., Peterson LB. 1995. Genetic control of autoimmune diabetes in the NOD mouse. *Ann Rev Immunol* 13: 179-200

135. Fujita, T., Yui, R., Kusumoto, Y., Serizawa, Y., Makino, S., Tochino, Y. 1982...

Lymphocytic insulitis in a 'non-obese diabetic (NOD)' strain of mice: an immunohistochemical and electron microscope investigation. *Biomed Res* 3: 429-443

136. Acha-Orbea H., McDevitt HO. 1987. The first external domain of the nonobese diabetic mouse class II I-A beta chain is unique. *Proc Natl Acad Sci* 84: 2435-9

137. Fugger L., Liang J., Gautam A., Rothbard JB., McDevitt HO. 1996. Quantitative analysis of peptides from myelin basic protein binding to the MHC class II protein, I-Au, which confers susceptibility to experimental allergic encephalomyelitis. *Mol Medicine* 2: 181-8

138. Reich EP., von Grafenstein H., Barlow A., Swenson KE., Williams K., Janeway CA Jr. 1994. Self peptides isolated from MHC glycoproteins of non-obese diabetic mice. *J. Immunol* 152: 2279-88

139. Cetkovic-Cvrlje M., Gerling IC, Muir A., Atkinson MA., Elliott, JF, Leiter, EH. Retardation or acceleration of Diabetes in NOD/Lt mice mediated by intrathymic administation of candidate beta cell antigens. *Submitted*

140. Kaufman DL., Clare-Salzler M., Tian J., Forsthuber T., Ting GS., Robinson P., Atkinson MA., Sercarz EE., Tobin AJ., Lehmann PV. 1993. Spontaneous loss of T-cell tolerance to glutamic acid decarboxylase in murine insulin-dependent diabetes. *Nature* 366: 69-72

141. Kim J., Richter W., Aanstoot HJ., Shi Y., Fu Q., Rajotte R., Warnock G., Baekkeskov S. 1993. Differential expression of GAD65 and GAD67 in human, rat, and mouse pancreatic islets. *Diabetes* 42:1799-808

142. Chao CC., McDevitt HO. 1997. Identification of immunogenic epitopes of GAD 65 presented by Ag7 in non-obese diabetic mice. *Immunogenetics* 46: 29-34

143. Zechel MA., Elliott JF., Atkinson MA, Singh B. Characterization of novel T cell epitopes on glutamic acid decarboxylase relevant in autoimmune responses in NOD mice. *Submitted*

144. Wicker LS., Chen SL., Nepom GT., Elliott JF., Freed DC., Bansal A., Zheng S., Herman A., Lernmark A., Zaller DM., Peterson LB., Rothbard JB., Cummings R., Whiteley PJ. 1996. Naturally processed T cell epitopes from human glutamic acid decarboxylase identified using mice transgenic for the type 1 diabetes-associated human MHC class II allele, DRB1*0401. *J. Clin. Invest.* 98: 2597-603

145. Hemler ME., Brenner MB., McLean JM., Strominger JL. 1984. Antigenic stimulation regulates the level of expression of interleukin 2 receptor on human T cells. *Proc Natl Acad Sci USA* 81: 2172-5

146. Foung SK., Sasaki DT., Grumet FC., Engleman EG. 1982. Production of functional human T-T hybridomas in selection medium lacking aminopterin and thymidine. *Proc Natl Acad Sci USA* 79: 7484-8

147. Atkinson MA., Maclaren NK. 1994. The pathogenesis of insulin-dependent diabetes mellitus. *N. Engl. J. Med.* 331: 1428-36

148. Patel SD., Cope AP., Congia M., Chen TT., Kim E., Fugger L., Wherrett D., Sonderstrup-McDevitt G. 1997. Identification of immunodominant T cell epitopes of human glutamic acid decarboxylase 65 by using HLA-DR(alpha1*0101,beta1*0401) transgenic mice. *Proc Natl Acad Sci USA* 94: 8082-7

149. Harrison LC., Honeyman MC., Trembleau S., Gregori S., Gallazzi F., Augstein P., Brusic V., Hammer J., Adorini L. 1997. A peptide-binding motif for I-A^{g7}, the class II major histocompatibility complex (MHC) molecule of NOD and Biozzi AB/H mice. *J. Exp. Med.* 185: 1013-21

150. Quinn A., Sercarz EE. 1996. T cells with multiple fine specificities are used by non-obese diabetic (NOD) mice in the response to GAD(524-543). *J. Autoimmunity* 9: 365-70

151. Lundin KE., Qvigstad E., Ronningen KS., Thorsby E. 1990. Antigen-specific T cells restricted by HLA-DQw8: importance of residue 57 of the DQ beta chain. *Hum Immunol* 28: 397-405

152. Letourneur F., Malissen B. 1989. Derivation of a T cell hybridoma variant deprived of functional T cell receptor alpha and beta chain transcripts reveals a nonfunctional alpha-mRNA of BW5147 origin. *Eur. J. Immunol* 19: 2269-74

153. Blank U., Boitel B., Mege D., Ermonval M., Acuto O. 1993. Analysis of tetanus toxin peptide/DR recognition by human T cell receptors reconstituted into a murine T cell hybridoma. *Eur. J. Immunol* 23: 3057-65

154. Sanderson, S., Shastri, N. 1994. LacZ inducible, antigen/MHC-specific T cell hybrids. *International Immunol* 6: 369-376

155. Shaw JP., Utz PJ., Durand DB., Toole JJ., Emmel EA., Crabtree GR. 1988. Identification of a putative regulator of early T cell activation genes. *Science* 241: 202-5

156. Fiering S., Northrop JP., Nolan GP., Mattila PS., Crabtree GR., Herzenberg LA. 1990. Single cell assay of a transcription factor reveals a threshold in transcription activated by signals emanating from the T-cell antigen receptor. *Genes & Development* 4: 1823-34

157. Harvey EN. *Bioluminescence*, New York: Academic Press, 1952

158. Inouye S., Tsuji FI. 1994. Aequorea green fluorescent protein. Expression of the gene and fluorescence characteristics of the recombinant protein. *FEBS Letters* 341: 277-80

159. Prasher DC., Eckenrode VK., Ward WW., Prendergast FG., Cormier MJ. 1992. Primary structure of the Aequorea victoria green-fluorescent protein. *Gene* 111: 229-33

160. Morin JG., Hastings JW. 1971. Energy transfer in a bioluminescent system. *J. Cell Physiol* 77: 313-8

161. Ward WW., Bokman SH. 1982. Reversible denaturation of Aequorea green-fluorescent protein: physical separation and characterization of the renatured protein. *Biochemistry* 21: 4535-40

162. Chalfie M., Tu Y., Euskirchen G., Ward WW., Prasher DC. 1994. Green fluorescent protein as a marker for gene expression. *Science* 263: 802-5

163. Ikawa M., Kominami K., Yoshimura Y., Tanaka K., Nishimune Y., Okabe M. Green fluorescent protein as a marker in transgenic mice. *Develop. Growth Differ.* 37: 455-459

164. Heim R., Cubitt AB., Tsien RY. 1995. Improved green fluorescence. *Science* 373: 663-4

165. Truneh A., Albert F., Golstein P., Schmitt-Verhulst AM. 1985. Early steps of lymphocyte activation bypassed by synergy between calcium ionophores and phorbol ester. *Nature* 313: 318-20

166. Crispe IN. 1994. Fatal interactions: Fas-induced apoptosis of mature T cells. *Immunity* 1: 347-49

167. Brunner T., Mogil RJ., LaFace D., Yoo NJ., Mahboubi A., Echeverri F., Martin SJ., Force WR., Lynch DH., Ware CF., *et al.* 1995. Cell-autonomous Fas (CD95)/Fas-ligand interaction mediates activation-induced apoptosis in T-cell hybridomas. *Nature* 373: 441-4

168. White J., Blackman M., Bill J., Kappler J., Marrack P., Gold DP., Born W. 1989. Two better cell lines for making hybridomas expressing specific T cell receptors. *J. Immunol.* 143: 1822-5

169. Barve SS., Cohen DA., De Benedetti A., Rhoads RE., Kaplan AM. 1994. Mechanism of differential regulation of IL-2 in murine Th1 and Th2 T cell subsets. 1. Induction of IL-2 transcription in Th2 cells by up-regulation of transcription factors with the protein synthesis initiation factor 4E. *J. Immunol.* 152: 1171-81

170. Donnadieu E., Trautmann A., Malissen M., Trucy J., Malissen B., Vivier E. 1994. Reconstitution of CD3 zeta coupling to calcium mobilization via genetic complementation. *J. Biol Chem* 269: 32828-34

171. Crameri A., Whitehorn EA., Tate E., Stemmer WPC. 1996. Improved green fluorescent protein by moelcular evolution using DNA shuffling. *Nature Biotechnology* 4: 315-19

172. Evavold BD., Sloan-Lancaster J., Allen PM. 1993. Tickling the TCR: selective T-cell functions stimulated by altered peptide ligands. *Immunol Today* 14: 602-9

173. Ausubel LJ., Krieger JI., Hafler DA. 1997. Changes in cytokine secretion induced by altered peptide ligands of myelin basic protein peptide 85-99. *J. Immunol* 159: 2502-12

174. Kalandadze A., Galleno M., Foncerrada L., Strominger JL., Wucherpfennig KW. 1996. Expression of recombinant HLA-DR2 molecules. Replacement of the hydrophobic transmembrane region by a leucine zipper dimerization motif allows the assembly and secretion of soluble DR alpha beta heterodimers. *J. Biol. Chem.* 271: 20156-62

175. Kozono H., White J., Clements J., Marrack P., Kappler J. 1994. Production of soluble MHC class II proteins with covalently bound single peptides. *Nature* 369: 151-4

176. Fremont DH., Hendrickson WA., Marrack P., Kappler J. 1996. Structures of an MHC class II molecule with covalently bound single peptides. *Science* 272: 1001-4

177. Pearson CI., van Ewijk W., McDevitt HO. 1997. Induction of apoptosis and T helper 2 (Th2) responses correlates with peptide affinity for the major histocompatibility complex in self-reactive T cell receptor transgenic mice. *J. Exp. Med.* 185: 583-99